

1 Article

2 **Mapping Fishing Activities and Suitable Fishing**  
3 **Grounds Using Nighttime Satellite Images and**  
4 **Maximum Entropy Modelling**5 **Rollan C. Geronimo<sup>1,2,\*</sup>, Erik C. Franklin<sup>1,3</sup>, Russell E. Brainard<sup>2</sup>, Christopher D. Elvidge<sup>4</sup>,**  
6 **Mudjekeewis D. Santos<sup>5</sup>, Roberto Venegas<sup>2</sup>, Camilo Mora<sup>1</sup>**7 <sup>1</sup> Department of Geography, University of Hawai'i at Mānoa, Honolulu, Hawai'i 96822, USA;  
8 cmora@hawaii.edu; erik.franklin@hawaii.edu9 <sup>2</sup> Ecosystem Sciences Division, Pacific Islands Fisheries Science Center, National Marine Fisheries Service,  
10 U.S. National Oceanic and Atmospheric Administration, Honolulu, Hawai'i 96818, USA;  
11 rusty.brainard@noaa.gov; roberto.venegas@noaa.gov12 <sup>3</sup> Hawaii Institute of Marine Biology, School of Ocean and Earth Science and Technology, University of  
13 Hawaii at Manoa, Kaneohe, Hawaii 96744 USA; erik.franklin@hawaii.edu14 <sup>4</sup> Earth Observation Group, National Oceanic and Atmospheric Administration's National Centers for  
15 Environmental Information, Boulder, Colorado 80305, USA; chris.elvidge@noaa.gov16 <sup>5</sup> National Fisheries Research and Development Institute, Quezon City, Metro Manila, Philippines;  
17 mudjesantos@gmail.com

18 \* Correspondence: rollan@hawaii.edu; Tel.: + 1-808-956-8465

19 Received: date; Accepted: date; Published: date

20 **Abstract:** Fisheries surveys over broad spatial areas are crucial in defining and delineating  
21 appropriate fisheries management areas. Yet accurate mapping and tracking of fishing activities  
22 remain largely restricted to developed countries with sufficient resources to use Automated  
23 Identification Systems and Vessel Monitoring Systems. **For most developing countries, the spatial  
24 extent and boundaries of fishing grounds are not completely known.** We used satellite images at  
25 night to detect fishing grounds in the Philippines for fishing gears that use powerful lights to attract  
26 coastal pelagic fishes. We used nightly boat detection data, extracted by U.S. NOAA from the Visible  
27 Infrared Imaging Radiometer Suite, for the Philippines from 2012 to 2016, covering 1,713 nights, to  
28 examine spatio-temporal patterns of fishing activities in the country. Using density-based  
29 clustering, we identified 134 Core Fishing Areas (CFAs) ranging in size from 6 to 23,000 km<sup>2</sup> within  
30 the Philippines' Contiguous Maritime Zone. The CFAs had different seasonal patterns and range of  
31 intensities in total light output, possibly reflecting differences in multi-gear and multi-species  
32 signatures of fishing activities in each fishing ground. Using maximum entropy modeling, we  
33 identified bathymetry and chlorophyll as the main environmental predictors of spatial occurrence  
34 of these CFAs when analyzed together, highlighting the multi-gear nature of the CFAs. Applications  
35 of the model to specific CFAs identified different environmental drivers of fishing distribution,  
36 coinciding with known oceanographic associations for a CFA's dominant target species. This case  
37 study highlights nighttime satellite images as a useful source of spatial fishing effort information  
38 for data-deficient fisheries, especially in Southeast Asia.39 **Keywords:** VIIRS; fisheries; maximum entropy; mapping  
40

41

## 42 1. Introduction

43 Monitoring and mapping of fishing activities are critical components of planning and  
44 management for marine fisheries [1]. Fishing location data have been used to identify and delineate  
45 fishing grounds [2], improve stock assessments [1,3], estimate fishing effort [4], and evaluate the  
46 impact of exclusion interventions in redistributing maritime activities [5]. Properly applying spatial  
47 catch-per-unit-effort data as indices of fish population abundance trends also require information on  
48 changes in spatial distribution of fishing effort [6]. With the increased call to manage fisheries within  
49 an ecosystem context, understanding the spatial dimension of fisheries becomes more crucial, from  
50 identification of fisheries management units to the development of appropriate and efficient  
51 management actions [7–9].

52 Despite its importance, spatial information on fishing activities remains sparse in developing  
53 countries due to the large number of fishing vessels and the high costs associated with collecting  
54 these data. Southeast Asian countries, for example, have some of the highest fishing effort densities  
55 (in boat-meters per km<sup>2</sup>) in the world [10], yet the majority of fishing vessels in this region do not  
56 have Automated Identification System (AIS) transceivers. A global mapping of fishing activities  
57 using AIS highlighted a clear and striking gap in fishing boat detections within the greater Southeast  
58 Asia [11]. Costs for setting up and maintaining vessel monitoring systems can be prohibitive,  
59 reaching in excess of U.S. \$1 million to equip 1,000 vessels and more than U.S. \$250,000 annually for  
60 maintenance [12]. With many developing countries having tens of thousands of fishing vessels, other  
61 complementary sources of spatial data for fisheries need to be explored.

62 Global nighttime satellite images offer an alternative source of spatial data for fisheries that use  
63 lights to attract shoaling fish [13–15]. The high intensity lights used by these fishing methods are  
64 identifiable from nighttime satellite images, which may then give important insights to fishing  
65 activities in data-poor areas. Maritime applications of nighttime satellite products include mapping  
66 light pollution in marine protected areas [16,17]; mapping offshore petroleum gas flares [18,19]; boat  
67 detection and tracking [20–22]; fish habitat suitability mapping [23,24]; estimating fishing effort and  
68 intensity for single species fisheries [23,25–27]; and mapping of current and predicted potential  
69 fishing areas / zones [24,28,29].

70 The quality and availability of nighttime satellite images have improved considerably, making  
71 it feasible to study fishing activities that use lights at night in greater detail. Compared to the  
72 nighttime satellites launched through the 40 year-old U.S. Defense Meteorological Satellite Program  
73 (DMSP), the Visible Infrared Imaging Radiometer Suite (VIIRS) instrument on-board the newer  
74 Suomi National Polar-orbiting Partnership satellite captures nighttime lights at much finer  
75 resolutions of 742 x 742 meters (vs. 5 x 5km); detects an order of magnitude of dimmer lights (~2 x 10<sup>-11</sup>  
76 Watts/cm<sup>2</sup>/sr vs. ~5 x 10<sup>-10</sup> Watts/cm<sup>2</sup>/sr); and has higher data quantization (14 bit vs. 6 bit) [30]. The  
77 increased quantization means that radiance values are stored as floating values with a much wider  
78 range than the 64 digital numbers available for DMSP-OLS, allowing for more precise measurements  
79 of light intensity.

80 Powerful lights are used extensively in Southeast Asia to attract schooling small pelagic fishes  
81 and squids, making them easier to enclose with nets and haul the catch or lure in with fish hooks. In  
82 the Philippines, the most common fishing gears using powerful lights are ring nets, purse seines, and  
83 boat-based lift nets (Table 1). In Indonesia, nighttime lights detected from the VIIRS Day/Night band  
84 matched with data from vessel monitoring systems for squid lift net and jigging and purse seine small  
85 pelagic fishing [31]. Weaker intensity lights are also used in association with fish aggregating devices  
86 for tuna [32] and in catching post-larval stages of small pelagic fishes using fine-meshed scoop nets  
87 [33].  
88

89

**Table 1.** Major fishing gears utilizing lights to attract fishes in the Philippines [34]

Gear	Target species	Description of light use
Ring net	Small scad, sardine, mackerel	200-500 watt bulbs (4-8 bulbs/boat) FADs: 500 watt bulbs (2-4 bulbs/FAD) or pressurized gas lamps
Small pelagic purse seine	Scad, mackerel, sardines	Incandescent 1000 watts/bulb (10-12 bulbs/boat) Halogen 1000-5000 watts/bulb (6-10 bulbs/boat)
Tuna purse seine	Skipjack tuna	FADs are lighted by a dim light boat which has 2-4 pieces of 1,000 watt bulbs. 10-20 halogen lights (1000-5000 watts/bulb)
Bag net or fish lift net	Roundscad, Anchovies, Indian sardines	Some use underwater metal halide lights Biggest found in Cavite, Quezon, Davao, and Zamboanga 19x1,000 watt bulbs or 2-8 units of high wattage metal halide bulbs (1,000-5,000 watts)
Commercial round haul seine	Anchovies Squids [35]	No details available on types of lighting used

90 We used data from the VIIRS satellite images to fill in crucial information gaps in the spatial  
 91 distribution of light-assisted fishing activities in the Philippines. Our objectives in this study are to:  
 92 (1) identify the Core Fishing Areas (CFA) based on the density of nighttime lights, (2) characterize  
 93 the spatio-temporal patterns in nighttime light-assisted fishing activities for each core fishing area,  
 94 and (3) produce fishing ground suitability maps based on the environmental conditions that  
 95 distinguish core fishing areas from non-core fishing areas.

## 96 2. Materials and Methods

### 97 2.1. VIIRS Boat Detection Data

98 Nightly VIIRS Boat Detection (VBD) data from April 1, 2012 to December 31, 2016 were  
 99 downloaded from the U.S. National Oceanic and Atmospheric Administration National Center for  
 100 Environmental Information's Earth Observation Group's website  
 101 ([https://www.ngdc.noaa.gov/eog/viirs/download\\_phil\\_boat.html](https://www.ngdc.noaa.gov/eog/viirs/download_phil_boat.html)). Individual VBD records  
 102 represent lit-up pixels in a VIIRS Day/Night Band image [21,31] for one night. The VBD data files  
 103 contain information on geo-location of lit-up pixels, radiance value (in nanoWatts/cm<sup>2</sup>/sr), date and  
 104 time the image was taken, quality flag, various thresholding values used to distinguish a potential  
 105 fishing vessel light source versus others, and corresponding VIIRS Day/Night Band image filename.  
 106 We extracted only VBD points with Quality Flags 1 (strong boat detection), 2 (weak boat detection),  
 107 3 (blurry boat detection), 8 (recurring lights), and 10 (weak and blurry lights), corresponding to  
 108 radiance spikes that are more likely from marine vessel light sources.



109 **When the satellite's pole-to-pole orbit,** some image granules can have zonal overlap especially  
 110 in mid to higher latitudes with a 2 to 3-hour time difference. To avoid double counting of VBD for  
 111 the same boat, we identified VBD from two overlapping granules that are 1 kilometer apart and  
 112 randomly selected one of the two points to represent the vessel's location for that night.

113 Since most of the fishing gears that use lights (Table 1) are catching coastal pelagic fishes [36],  
 114 we limited our analyses to VBD within the Philippines' 24-nautical mile contiguous zone [37].

### 115 2.2. Identification of Core Fishing Areas



116 While fishing activities can occur anywhere in the ocean, previous studies have shown that  
 117 fishers tend to cluster highly at specific marine locations [38,39]. Initial inspection of VIIRS Boat  
 118 Detection data revealed similar patterns in the Philippines. We thus defined these areas as Core

119 Fishing Areas (CFAs) or locations which are repeatedly visited and where there is dense fishing  
120 activity.


121 We accounted for the visitation frequency by creating a  standardized 700-meter resolution grid  
122 and counting the number of years when VBD was detected in each grid cell. **We only used the VBD**  
 **data within cells that had more than 1 year of VBD occurrence.** This also removed a lot of widely  
123 scattered lights. We then obtained the centroid coordinates of each cell with more than 1 year of VBD  
124 data and ran a series of Hierarchical Density-Based Spatial Clustering of Applications with Noise  
125 (HDBSCAN) [40] using different parameter combinations of “minimum cluster size” (i.e., 3 to 30)  
126 and “minimum samples” (i.e., 3 to 35), resulting in 1,200 different clustering combinations. We  
127 selected the clustering parameter combination that yielded the least number of points classified as  
128 “noise” while maintaining reasonable clustering of known small pelagic fish (SPF) fishing areas (e.g.,  
129 Northeastern Palawan round scad fishing grounds; Tayabas Bay fisheries; and Basilan strait sardine  
130 fisheries). Concave hull polygons were estimated for each cluster of points using a Delaunay  
131 Triangulation algorithm to visualize the clusters. Finally, using high resolution images from Google  
132 Earth and shipping traffic data from <https://www.marinetraffic.com/> as reference (Figure S1), we  
133 developed a raster mask to removed polygons in areas with possible high occurrence of non-fishing  
134 related shipping activities (e.g., around busy harbors, shipping lanes, and areas with mining activities  
135 near the coast) since VBD points in these high-traffic areas could include a large number of non-  
136 fishing vessels that turn on additional deck and navigational lights. This mask was also used for the  
137 MaxEnt modeling of suitable fishing grounds based on annual VBD occurrence. Annual raster  
138 overlays were done using R (v. 3.5.1, R Development Core Team) [41], while hierarchical density-  
139 based spatial clustering of applications with noise [42] and concave hull estimations were ~~ran~~  
140 using Python 2.7 ([www.python.org](http://www.python.org)).  
141

### 142 2.3. Clustering CFAs based on monthly patterns and radiance values of VBDs

143 Each CFA can be characterized by the composition of fishing gears operating in the area and the  
144 seasonal patterns in fishing. Multiple light-assisted fishing gears (Table 1) most likely operate in each  
145 fishing ground. Radiance values can be used as a relative measure of light source intensity with  
146 higher radiance corresponding to brighter lights [43]. A narrow radiance range could imply  
147 dominance of a single type of fishing gear while a wide range could mean that multiple gears are  
148 operating in the area. Seasonal patterns in fishing activities, on the other hand, could be defined by  
149 the mean nightly VBD by month, averaged across years within each CFA.

150 For radiance values, we applied histogram-valued data analysis based on the L2 Wasserstein  
 metric between distributions on log-transformed radiance per CFA [44]. **We limited this analysis to**  
151 **VBD points within CFAs occurring during nights with less than 50% moon illumination and less than**  
152 **50% cloud cover since both factors are known to affect recorded radiance beyond this percentage**  
153 **[21,43] (Figure S2).** Clustering was performed using the R Package “HistDAWass” [45]. For seasonal  
154 patterns in fishing activities within each CFA, we used the mean nightly VBD by month, averaged  
155 across years, and standardized the values between 0 and 1, corresponding to the minimum and  
156 maximum mean nightly VBD count by month.  As were grouped based on hierarchical clustering  
157 using Ward’s linkage method [46].  
158

### 159 2.4. MaxEnt modeling to identify environmental covariates with CFAs

160 We identified key environmental attributes that define Core Fishing Areas and used these  
161 relationships to map out other areas in the Philippines that have similar environmental attributes.  
 **Our main assumption is that environmental conditions can be used to partially predict the suitability**  
162 **of a given area for catching small pelagic fishes using light-assisted fishing methods. The relative**  
163 **abundance of target species plays a key role in the selection of fishing grounds by fishers.** Spatial  
164 distribution of small pelagic fishes has been known to correlate with various environmental attributes  
165 that link with food availability and habitat suitability.

166 We applied MaxEnt version 3.4.1 [47], a machine learning algorithm based on the concept of  
167 maximum entropy [48], to determine the environmental conditions that characterize Core Fishing  
168

169 Areas and identify other areas in the country with similar suitable environmental conditions that  
 170 could also have high fish productivity. Since the VIIRS satellite only takes one image per night and  
 171 small pelagic fishes are also caught using other gears that do not employ powerful lights, we  
 172 conservatively treated the VBD locations as presence-only data and randomly derived pseudo-  
 173 absences or background locations outside the CFAs. MaxEnt is one of the few models available that  
 174 can handle presence-only data and has been used extensively for species distribution modeling  
 175 [49,50]. It estimates the relative suitability of one place versus another by comparing conditional  
 176 density of covariates at presence sites with unconditional density of covariates across the study area  
 177 [51]. Probability of occurrences are returned which is relative to the “typical” conditions generated  
 178 from available presence points.

179 We applied MaxEnt at an aggregated 4 km resolution to match the resolution of remotely-sensed  
 180 environmental datasets used as predictors (Table 2). The model domain is the Philippines’ 24 nautical  
 181 mile contiguous zone bounded from 4° to 22° North and from 116° to 128° East. “Presence” locations  
 182 were defined as the centroid coordinates of 4-km grid cells that had VBD data and were inside any  
 183 of the CFAs for the periods 2013 to 2016. VBD data for 2012 was incomplete (i.e., starting only in April  
 184 2012) so it was not used in the MaxEnt models. Background points (~10,000) were randomly selected  
 185 within the model domain. The default regularization parameter of 1 was used to minimize model  
 186 over-fitting. “Maximum iterations” was set at 500. The “auto feature” selection method was also used  
 187 to allow MaxEnt to determine the appropriate feature class (e.g., linear, quadratic, product, threshold,  
 188 or hinge) [51] for each environmental predictor.

189 We collated environmental covariates commonly associated with the distribution of small  
 190 pelagic fishes [52–55] (Table 2). Gridded bathymetry was downloaded from the General Bathymetric  
 191 Chart of the Oceans (GEBCO) website. Monthly netCDF files for the other environmental predictors  
 192 (i.e., chlorophyll-a and sea surface temperature from MODIS; sea surface salinity, mixed layer  
 193 thickness, and sea surface height from the HYCOM hydrodynamic model) were downloaded from  
 194 the NOAA Coast Watch’s Environmental Research Division’s Data Access Program archives for the  
 195 years 2013 to 2016. Climatological and annual means were calculated for each predictor across the 4  
 196 years. All raster layers were projected to a Behrmann’s equal area projection at 4km resolution using  
 197 bilinear interpolation under the ‘raster’ package in R [56].

198 **Table 2.** Data used for the MaxEnt modeling of Core Fishing Areas.

Predictor	Original resolution	Units	Source
VIIRS Boat Detection	742m	--	NOAA Earth Observation Group ( <a href="https://ngdc.noaa.gov/eog/viirs/download_boat.html">https://ngdc.noaa.gov/eog/viirs/download_boat.html</a> )
Bathymetry	30 arc-sec	meters	GEBCO ( <a href="https://www.gebco.net/data_and_products/gridded_bathymetry_data/gebco_30_second_grid/">https://www.gebco.net/data_and_products/gridded_bathymetry_data/gebco_30_second_grid/</a> )
Sea surface temperature	4km	°C	MODIS-AQUA from NOAA CoastWatch ( <a href="https://coastwatch.pfeg.noaa.gov/erddap/index.html">https://coastwatch.pfeg.noaa.gov/erddap/index.html</a> )
Surface chlorophyll-a		mg/cm <sup>3</sup>	
Sea surface salinity		psu	
Mixed layer thickness (at density change of 0.03kg/m <sup>3</sup> )	1/12° (~9km)	meters	HYCOM + NCODA Global 1/12° Analysis ( <a href="https://coastwatch.pfeg.noaa.gov/erddap/index.html">https://coastwatch.pfeg.noaa.gov/erddap/index.html</a> )
Sea surface height		meters	

## 199 2.5. MaxEnt Scenarios

200 Using the biomod2 package in R [57], we ran three different sets of MaxEnt models and  
 201 scenarios: (a) climatology, (b) annual, and (c) specific CFAs (Table 3). For the climatology runs, we  
 202 generated time-series averaged rasters for all five dynamic predictors (i.e., except bathymetry) from  
 203 2013 to 2016. Under this set, models were run with and without bathymetry as a predictor and



204 accounting for possible effects of monsoons which have been known to affect small pelagic fish  
205 production in the Philippines [58].

206 The exact location of fishing activities, even within the same CFA, often changes across years.  
207 To account for annual variability of dynamic predictors on annual aggregated locations of VBD inside  
208 CFAs, we developed annual MaxEnt models from 2013 to 2016, using respective annual VBD data  
209 and annual averages for each predictor. Since the CFAs most likely differ in terms of the fishing fleet  
210 composition and targeted fish species, we selected two CFAs for which the dominant target species  
211 group is known and where most fishing gears that use lights are almost exclusively targeting these  
212 species. These CFAs are (a) the round scad fishery in Northeastern Palawan island (CFA # 106 in  
213 Figure 3) and (b) the sardine fisheries in the Sulu Archipelago (CFA # 70).

214 To identify other areas within the Philippines' 24 nautical mile contiguous zone with similar  
215 environmental characteristics to delineated CFAs, we generated predicted CFA suitability maps for  
216 all 10 MaxEnt models. Mean predicted suitability values per model was generated from suitability  
217 maps produced in each of the cross-validation runs (n=10 per model). The resulting suitability  
218 distributions were compared with the location of existing CFAs.

219 **Table 3.** MaxEnt models implemented

Model Name	Description
A. Climatology	
A1. Full	All VBD points within CFAs and mean climatology for all six environmental predictors
A2. Full – No Bathymetry	Bathymetry variable removed
A3. Northeast Monsoon (NEM)	Northeast monsoon model. VBD presence data limited to months within this monsoon period (i.e., November to April). Environmental predictors were averaged for Northeast monsoon months from 2013 to 2016.
A4. Southwest Monsoon (SWM)	Southwest monsoon model. VBD presence data limited to months within this monsoon period (i.e., May to October). Environmental predictors were averaged for Southwest monsoon months from 2013 to 2016.
B. Annual	
B1. 2013	All environmental predictors and VBD in CFAs for 2013
B2. 2014	All environmental predictors and VBD in CFAs for 2014
B3. 2015	All environmental predictors and VBD in CFAs for 2015
B4. 2016	All environmental predictors and VBD in CFAs for 2016
C. CFAs	
C1. Northeast Palawan	VBD in CFA # 106 (Northeast Palawan; Figure 3) and climatology of environmental predictors
C2. Sulu	VBD in CFA # 70 (Sulu; Figure 3) and climatology of environmental predictors

## 220 2.6. Model Validation and Evaluation

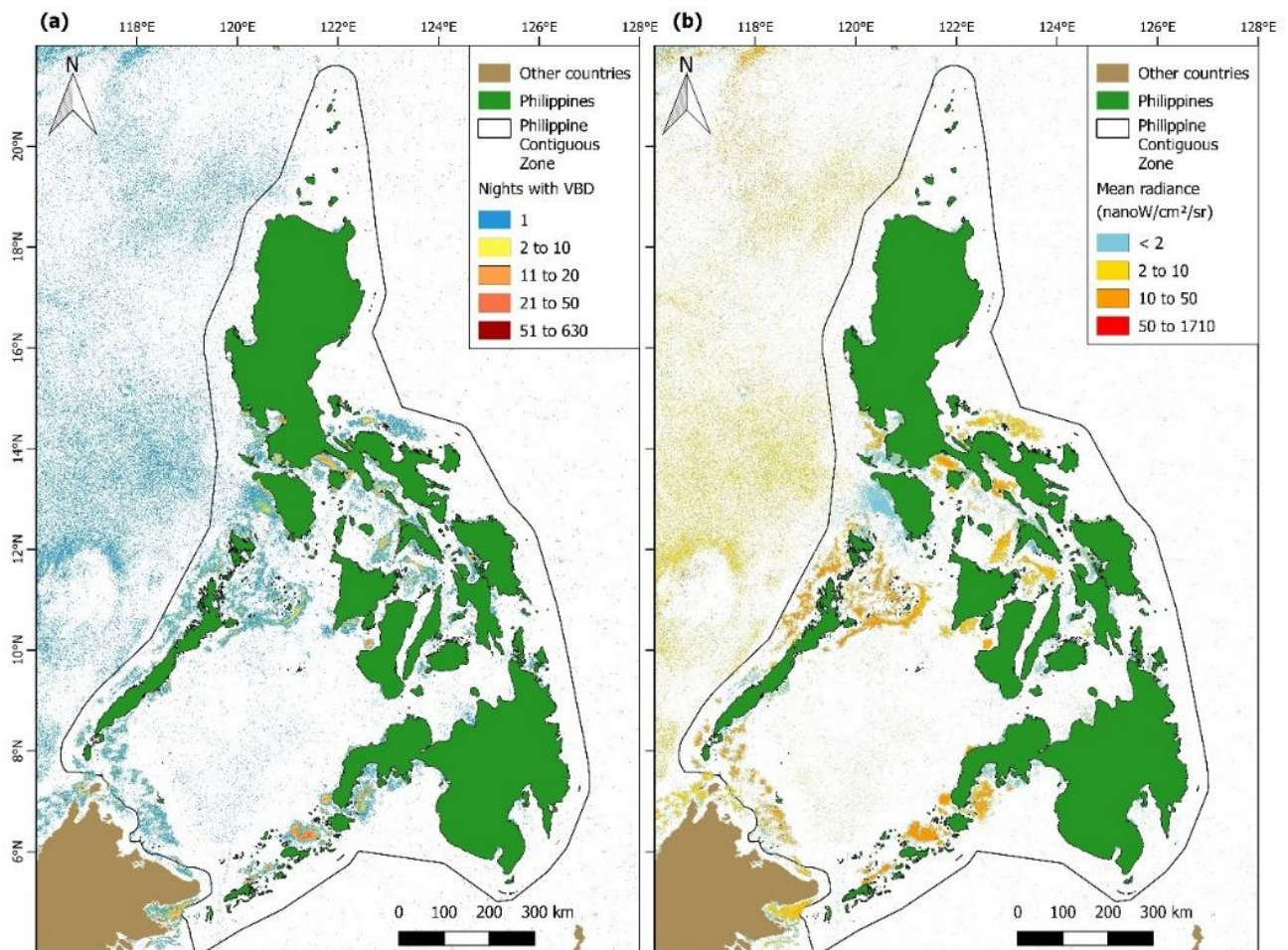
221 To test each MaxEnt model's predictive accuracy, we applied two repetitions of a 5-fold cross-  
222 validation that splits the presence data into five subsets. For each run, four of the five subsets (i.e.,  
223 80% of presence data) were aggregated and used to train the model, the remaining subset (i.e., 20%  
224 of presence data) was used to evaluate how well the trained model can accurately predict these  
225 occurrences [59]. Results were averaged across the repeated 5-fold cross-validation runs to predict

226 the current distribution of suitable fishing grounds for light-assisted fisheries within the Philippines'  
 227 24-nautical mile contiguous zone. Accuracy was measured for each cross-validation run using the  
 228 area under the curve of the receiver operating characteristic (AUC) and the true skill statistic (TSS)  
 229 [60–62]. AUC and TSS values range from 0 to 1. AUC values greater than 0.5 indicate that model  
 230 predictions are better than random predictions. TSS values greater than 0.4 indicate good models  
 231 [63].

232 We reported “variable importance” as a measure of the contribution of variables to the  
 233 discrimination of presence and pseudo-absence points. We also ran jackknife tests of environmental  
 234 importance (i.e., leave-one-out) which identifies improvements in model fit by adding or removing  
 235 each individual variable and measuring changes in training or testing data gain. Response curves  
 236 were generated and examined to derive the preferred range of environmental variables of potential  
 237 fishing areas.

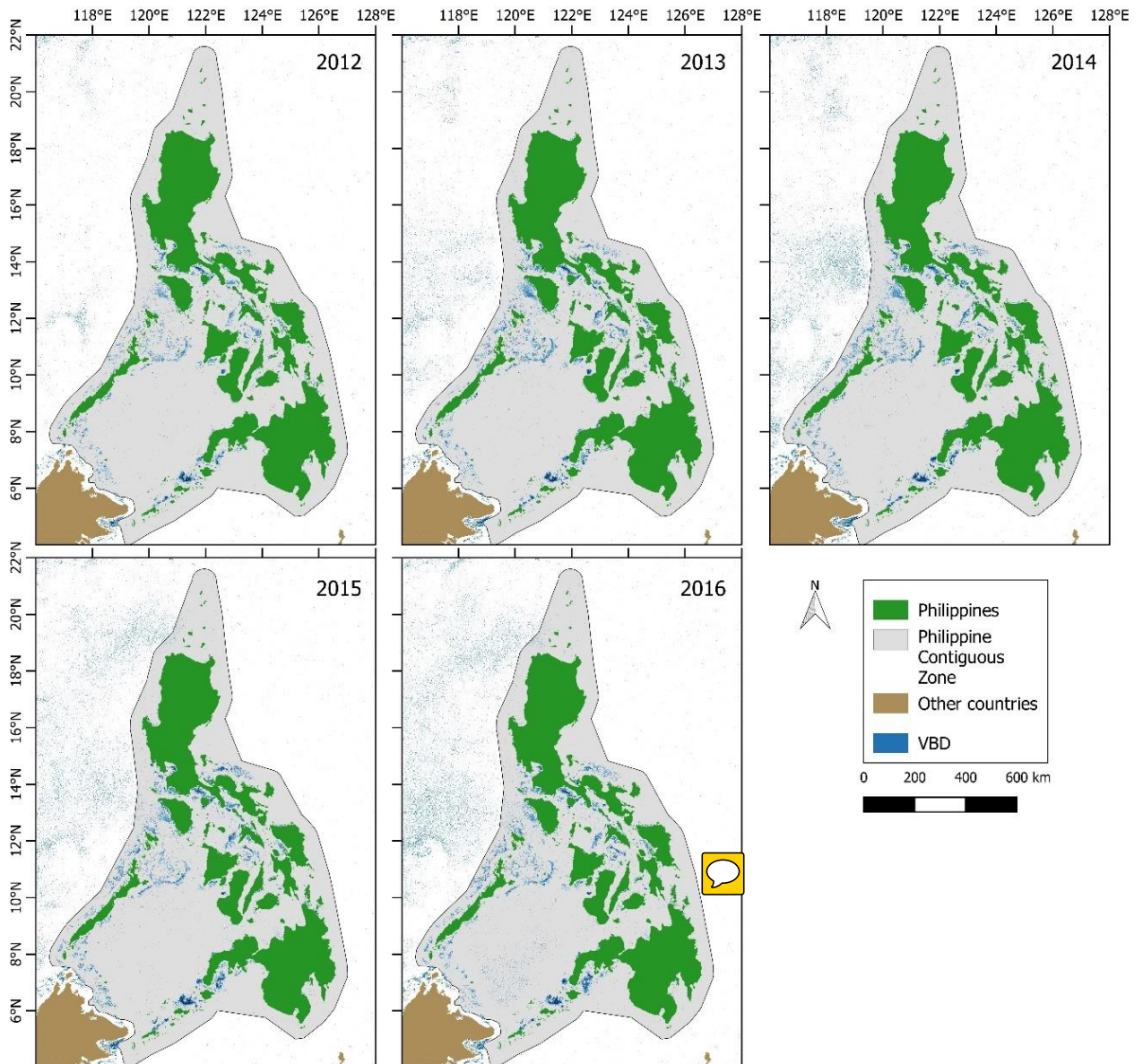
### 238 3. Results

239 VIIRS Boat Detection (VBD) locations within the Philippine’s 24-nautical mile contiguous zone  
 240 are highly clustered with specific areas being frequently visited (Figure 1a). Spatial patterns are also  
 241 apparent in terms of mean radiance values with most VBD locations having radiance values greater  
 242 than 2.0 nanoW/cm<sup>2</sup>/sr (Figure 1b). VBD with less than 2.0 radiance values are clearly clustered  
 243 together in some areas. Across years, the spatial patterns of VBD aggregations within the Philippines  
 244 has not change greatly across the years from 2012 to 2016 (Figure 2).



245

246 **Figure 1.** VIIRS Boat Detection (VBD) data from April 1, 2012 to December 31, 2016 aggregated on a  
 247 700m x 700m resolution grid showing (a) number of VBD detection per pixel over 1,713 nights and  
 248 (b) mean radiance value. The 24 nautical mile contiguous zone shapefile for the Philippines came from  
 249 Flanders Marine Institute’s Marine Regions database [37].



250

251

**Figure 2.** Annual rasters of VIIRS Boat Detections (VBD) with 700m x 700m grid resolution.

252

### 3.1. Core Fishing Areas in the Philippines Maritime Contiguous Zone

253

A total of 694,793 VBD points was recorded within the Philippines' contiguous zone over 1,713 nights. Eighty-five percent (85%) of these data points were in cells that were visited for at least 2 years over the 5-year period (Figure 3).

256

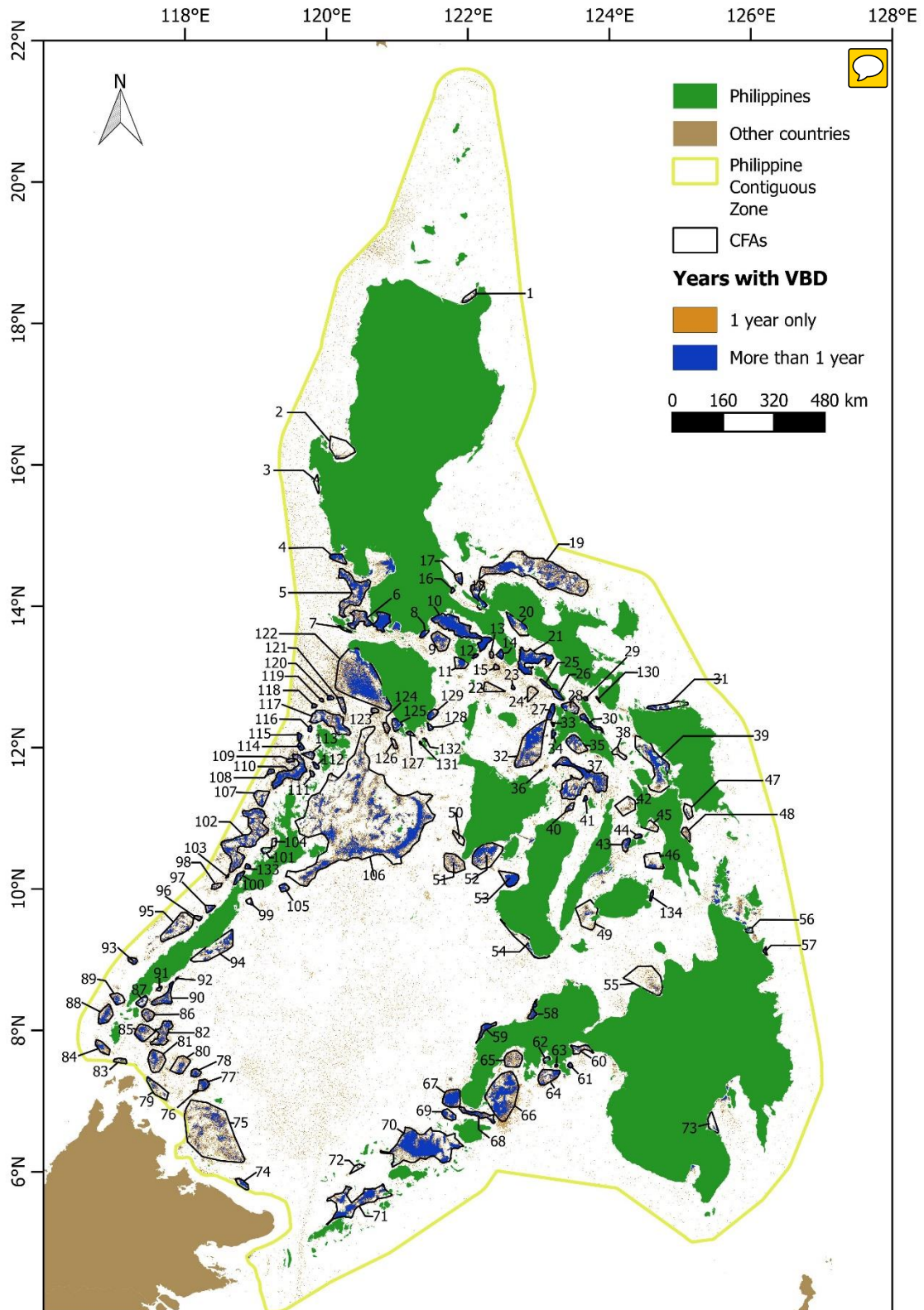
We identified 134 Core Fishing Areas (CFA) for light-assisted fishing in the Philippines based on HDBSCAN results using a "minimum cluster size" of 4 and "minimum samples" value of 25 (Figure 3; S1). This HDBSCAN parameterization initially labelled 94% of the frequently visited VBD cell centroids into 160 clusters. We removed clusters that were (a) too small, (b) includes or are located near major ports / piers, and/or (c) located in major shipping lanes.

261

The 134 CFAs ranged in size from 5.6 km<sup>2</sup> to 23,215 km<sup>2</sup> with a mean size of 700 km<sup>2</sup>. The maximum number of VBD for a given night was detected in March 3, 2014 with 1,124 lit-up pixels within the entire Philippines Contiguous Zone, 87% or 974 of these pixels were within CFAs. Per CFA, the maximum number of lights detected for a single night ranged from 2 to 227.

265



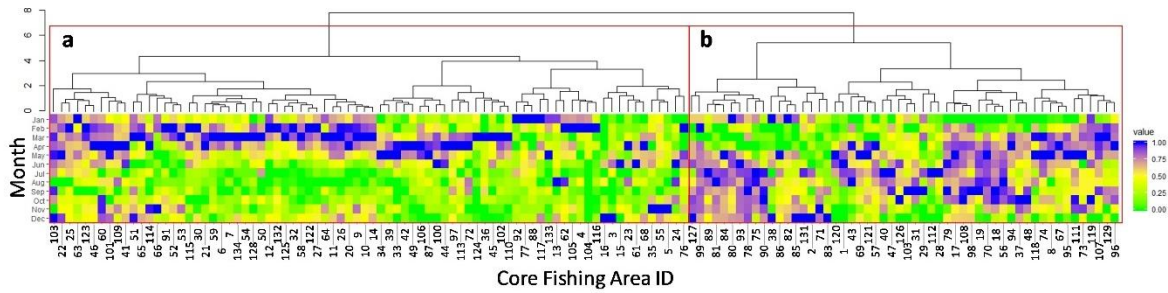


266

267 **Figure 3.** Core Fishing Areas (n=134) identified from HDBSCAN and after removing clusters in areas  
 268 that overlap with significant vessel traffic and close to major ports and piers, including mining jetties.  
 269 Details for each CFAs and corresponding names can be found in Table S1.

270

271 Seasonal patterns in fishing activity data varied per CFA (Figure 4; Figure S6-a). Cluster analyses  
 272 applied to averaged monthly VBDs showed two different groups based on the months when peak  
 273 fishing activity occur, generally corresponding with the monsoon months: (a) northeast monsoon  
 274 (November to April) and (b) southwest monsoon (May to October).

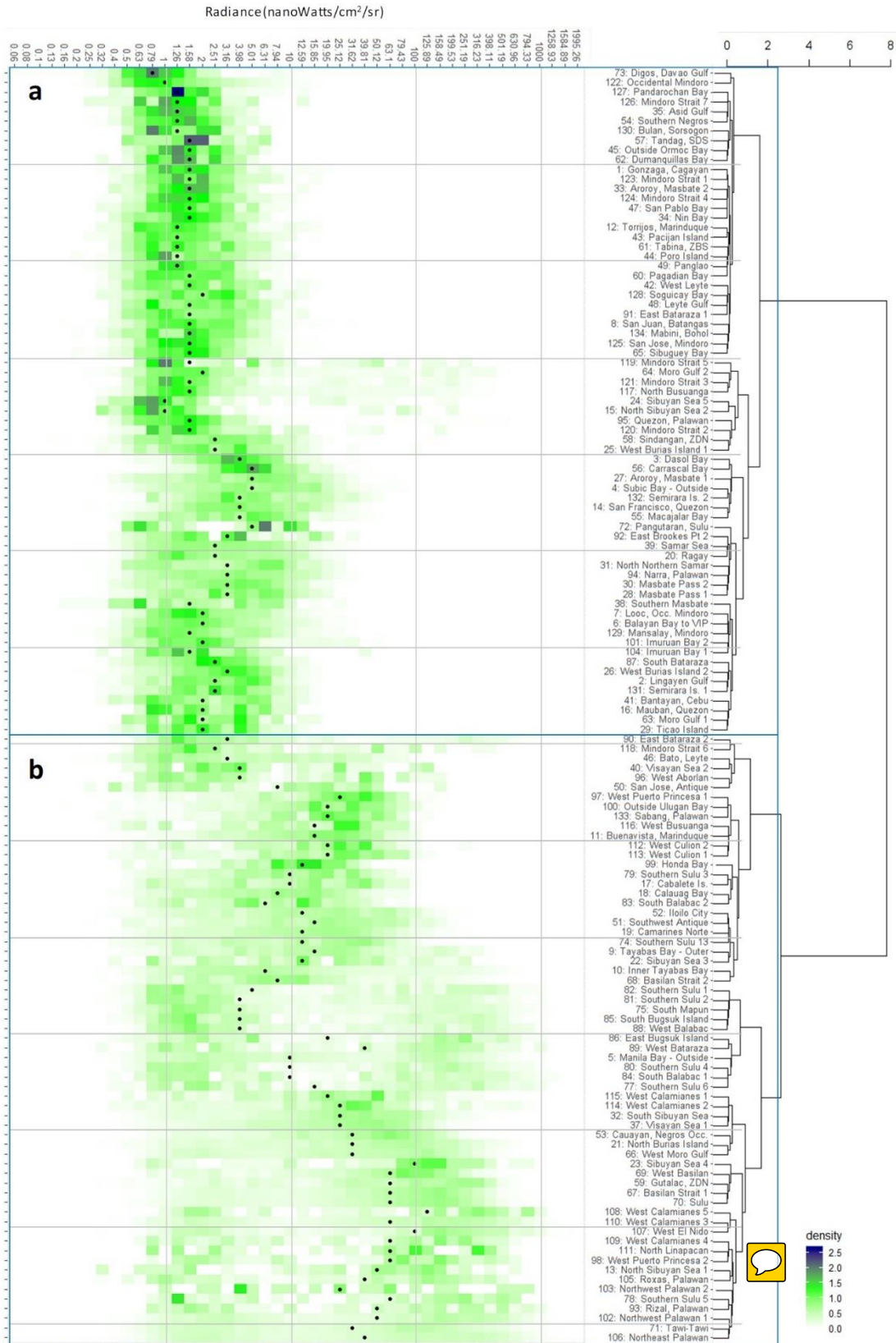


275  
 276 **Figure 4.** Hierarchical clustering of Core Fishing Areas based on scaled mean nightly VBD counts per  
 277 month using Ward’s linkage method showing two groups based on months of peak fishing activity:  
 278 (a) southwest monsoon (May to October) and (b) northeast monsoon (November to April).



280 Mean radiance values per CFA ranged from 1 to 166 nanoWatts/cm<sup>2</sup>/sr (Figure 5; Table S1).  
 281 Hierarchical clustering on radiance distribution values per CFA identified two distinct groups (h  
 282 cutoff = 5): (a) low radiance values (group mean = 3.4 nanoWatts/cm<sup>2</sup>/sr) and (b) high radiance values  
 (group mean = 61.2 nanoWatts/cm<sup>2</sup>/sr; Figure 5; Figure S6-b).

283



284

285

286

287

288

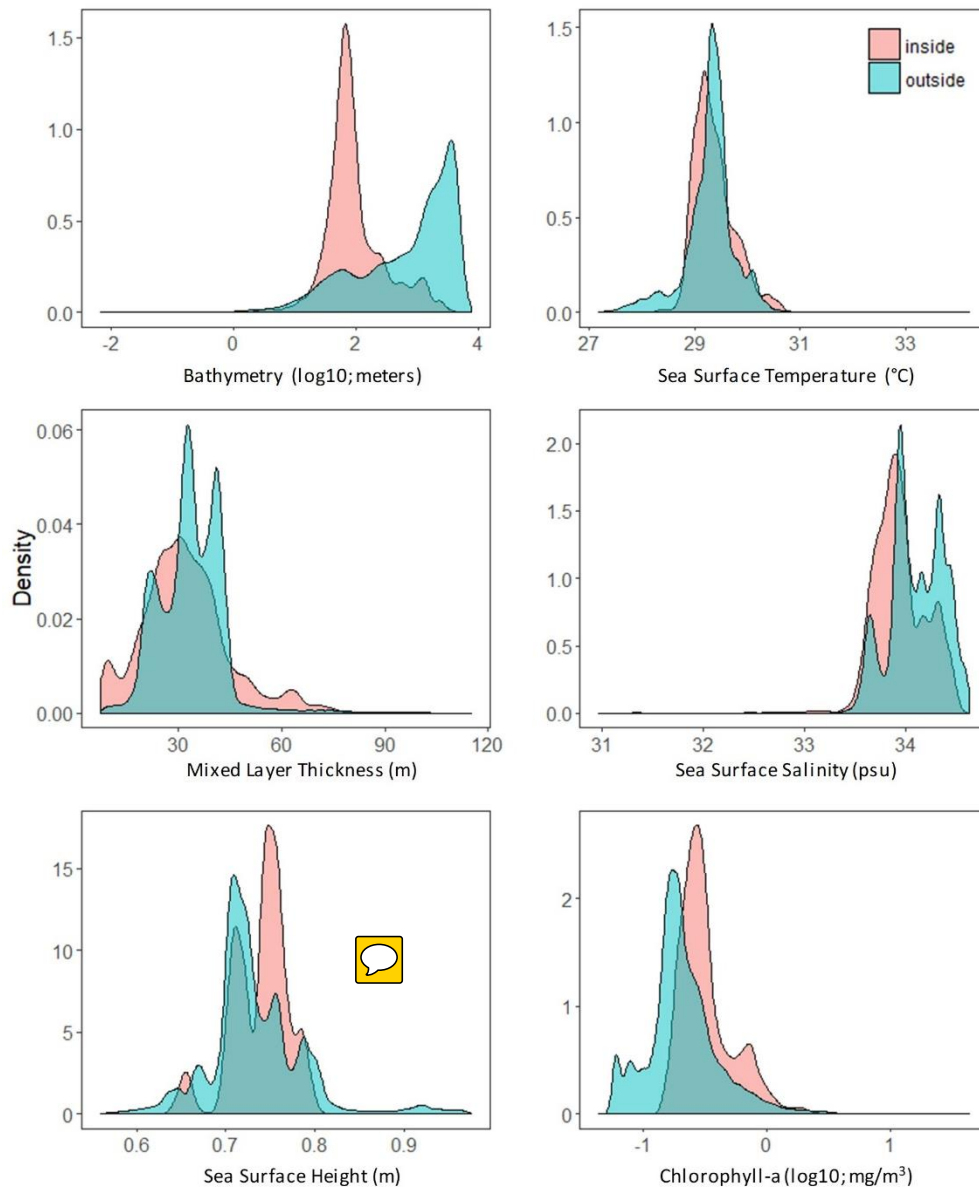
289

290

**Figure 5.** Hierarchical clustering of log-10 histograms of radiance values by CFA for nights with less than 50% moon illumination and cloud cover. Colors represent probability density of radiance bin per CFA. High-level groupings (around blue box) are based on spread of values with group (a) indicating high kurtosis, narrow range and low radiance values while group (b) are high radiance values with large spread and even some double peaks.

## 291 3.2. VBD and Environmental Variables

292 Mean sea surface temperature, chlorophyll-a, and bathymetry inside the CFAs differed from  
 293 those outside (Figure 6). CFAs have mean depth ranging between 5 meters and 1480 meters, mean  
 294 sea surface temperature between 28.5°C and 30.6°C, and mean surface chlorophyll-a values between  
 295 0.2 mg/m<sup>3</sup> and 2.2 mg/m<sup>3</sup>. The difference between monsoons are apparent only in mean chlorophyll  
 296 concentrations with the VBD points during the southwest monsoon located in areas with higher mean  
 297 chlorophyll-a concentrations (0.75mg/m<sup>3</sup> for Southwest Monsoon vs. 0.43mg/m<sup>3</sup> for Northeast  
 298 Monsoon; Welch Two Sample t-test  $p < 0.01$ ).



299

300 **Figure 6.** Density distribution of environmental predictors inside CFAs (red) versus outside (blue)  
 301 within the Philippines' 24 nautical mile contiguous zone. Bathymetry and chlorophyll-a values log-  
 302 10 transformed for clarity. Non-transformed values were used in the MaxEnt models.

303 All MaxEnt models performed better than random (i.e., AUC > 0.5 and TSS > 0.4; Table 4).  
 304 Among all the models, the one without bathymetry had the lowest AUC and TSS scores. The full  
 305 climatology, monsoonal, and annual models all had identical accuracy scores. The CFA-specific  
 306 models performed **very well, with very high AUC and TSS scores**. However, this is to be expected  
 307 given the restricted spatial extent of the VBD points used in these models.

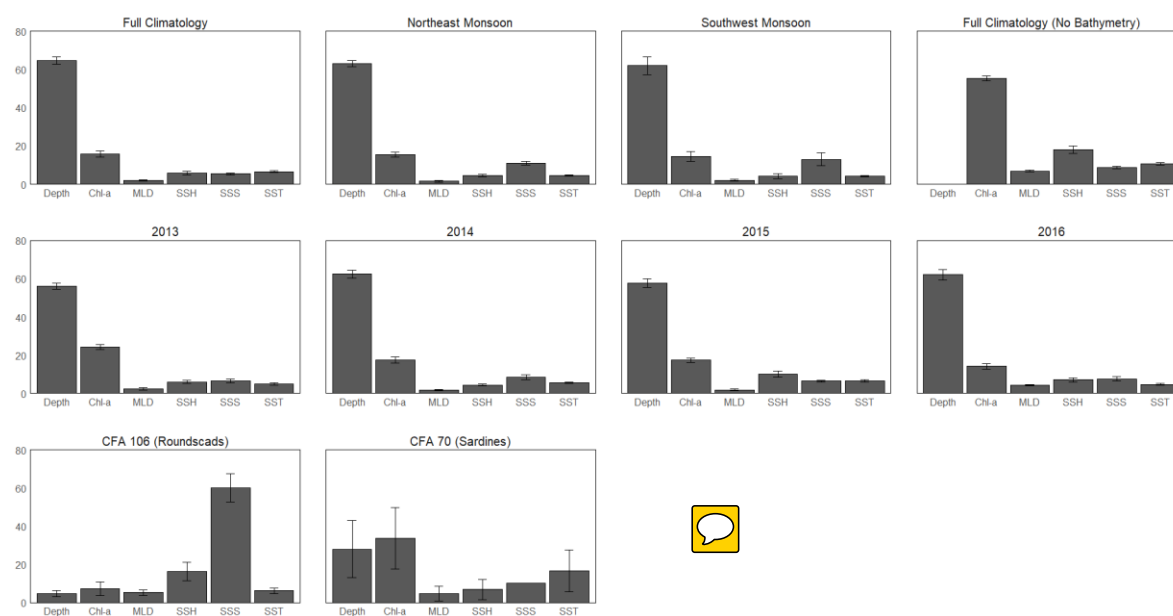


308

**Table 4.** Model evaluation scores for the different MaxEnt models.

Model	AUC	TSS
Full Climatology	0.88	0.59
Full – no Bathymetry	0.86	0.55
Northeast Monsoon	0.87	0.58
Southwest Monsoon	0.88	0.59
2013	0.89	0.61
2014	0.88	0.60
2015	0.89	0.62
2016	0.88	0.59
Northeast Palawan	0.94	0.87
Sulu	0.93	0.87

309 Bathymetry ranked highest in variable importance among all non-CFA-specific models, with  
 310 permutation importance values ranging from 56% (2013) to 64% (Full model) (Figure 7). This was  
 311 followed by chlorophyll-a with permutation importance ranging from 14% (2016) to 24% (2013). In  
 312 the model without bathymetry, chlorophyll explained most of the difference between CFA and non-  
 313 CFA locations with a mean permutation importance of 55%. Jackknife tests also identified bathymetry  
 314 as the variable with the highest model training, testing, and AUC gain when used in isolation (i.e.,  
 315 most useful information by itself) and the greatest decline in gain when removed from the model  
 316 (i.e., contains most information that is not present in the other variables). Sea surface salinity ranked  
 317 third in terms of variable permutation importance, particularly in the monsoonal models. Sea surface  
 318 temperature and sea surface height varied in their contributions to the model but mostly at less than  
 319 10% importance. In contrast to this general pattern, the variables contributing to the CFA-specific  
 320 models were more even with bathymetry ranking lowest in importance for the round scad fishery in  
 321 Northeast Palawan (CFA # 106). In the Northeast Palawan model, sea surface salinity ranked highest  
 322 in importance (60%) followed by sea surface height (16%). In the Sulu CFA model, chlorophyll-a  
 323 ranked highest in permutation importance (34%) followed by bathymetry (28%), sea surface  
 324 temperature (17%), and sea surface salinity (10%).



325

326

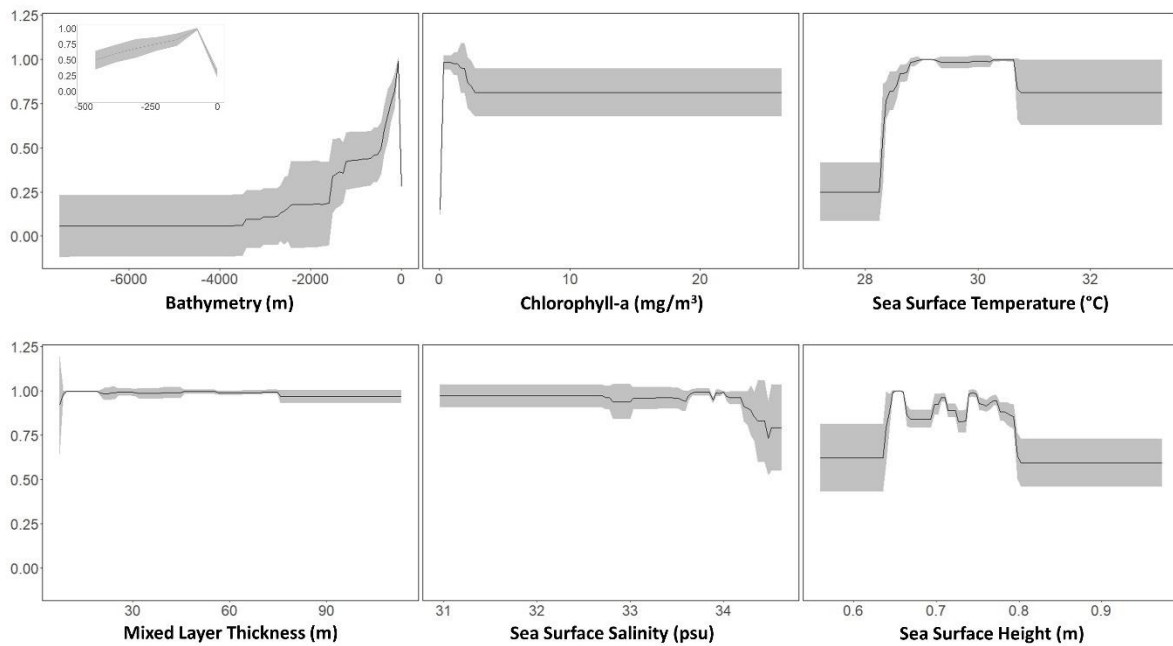
327

328

329

**Figure 7.** The relative contribution of different environmental predictors in determining the overall fit of the MaxEnt models to the VBD presence data used (normalized to percentages). Values averaged across two replicates of five-fold cross-validation runs of each MaxEnt model. Error bars are  $\pm 1$  standard deviation.

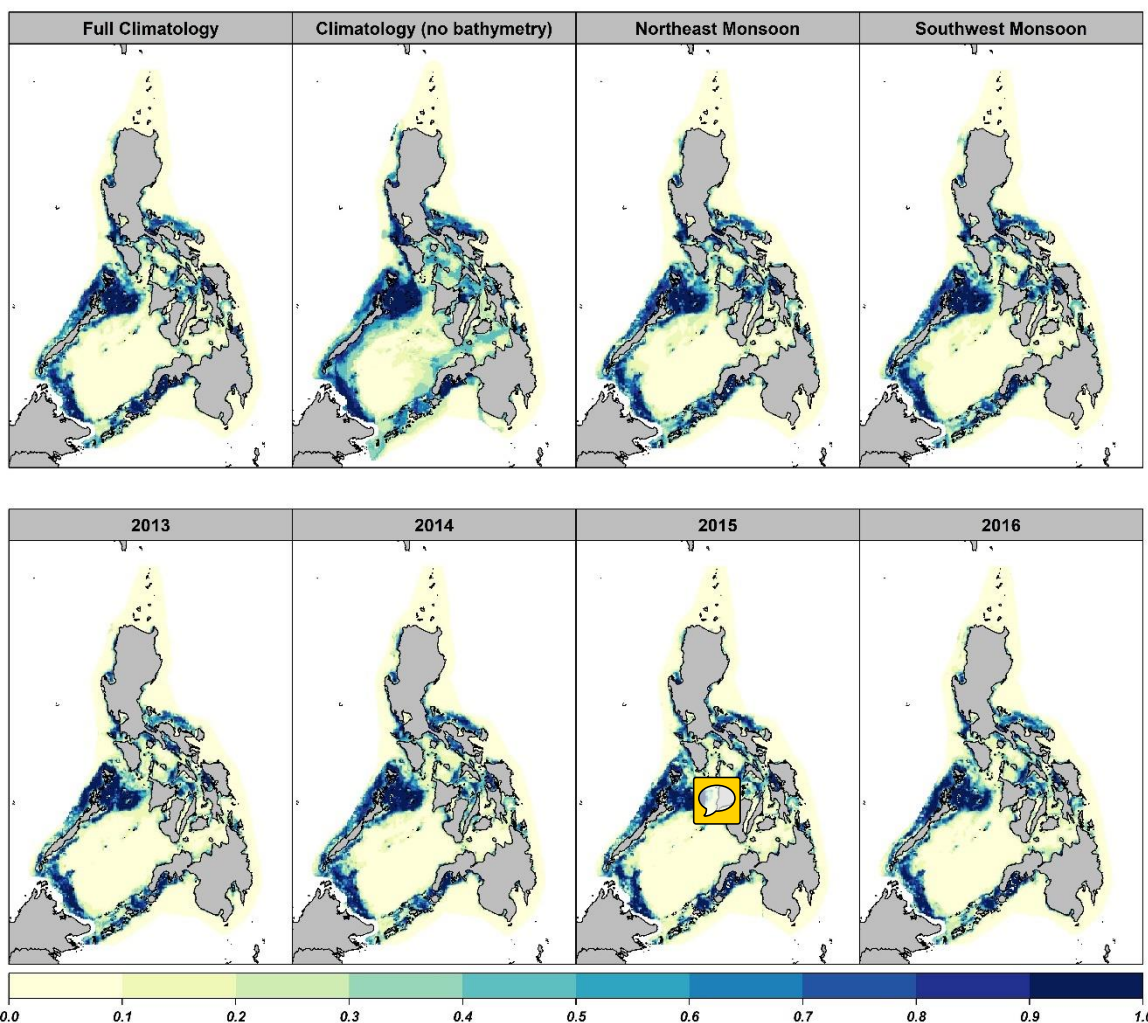
330 Model derived preferred ranges for the MaxEnt full climatology model are shown in Figure 8.  
 331 These response curves are marginal values showing the probability of occurrence of a site being a  
 332 Core Fishing Area with changing values of one variable while keeping all other variables at their  
 333 average sample value [64]. The logistic output or probability of occurrence increases with depth from  
 334 the shallowest depths up to around 100 meters then decrease rapidly to depths of 500 meters and  
 335 gradually declines further with depths deeper than 4000 meters. It peaked with chlorophyll-a values  
 336 between 0.3 and 2.0 mg/cm<sup>3</sup>. Frequently visited fishing sites also occurred more in areas with sea  
 337 surface temperatures between 28.6°C and 30.6°C. The effect of sea surface salinity, sea surface height,  
 338 and mixed layer thickness in discriminating CFA versus non-CFA areas was smaller compared to the  
 339 first three variables mentioned as indicated by the almost flat response across their entire range of  
 340 values.



341

342 **Figure 8.** Response curves per environmental predictor for the Full Climatology MaxEnt model  
 343 showing how each environmental variable affects the MaxEnt logistic prediction. Black lines show  
 344 the mean response of the two replicate 5-fold cross-validation runs. Shading represents  $\pm 1$  standard  
 345 deviation. Inset: Response curve for bathymetry with x-axis minimum truncated to 500m depth.

346 The predicted suitability of marine areas for light-assisted fishing based on the climatology and  
 347 annual MaxEnt models are shown in Figure 9. Predicted suitable areas with environmental  
 348 conditions typical of the CFAs are found in shallow, nearshore areas around existing CFAs. Predicted  
 349 suitable areas do not vary greatly across monsoons and years. For the CFA-specific MaxEnt models,  
 350 we found highly constrained areas of high suitability (Figure 10). However, the predicted areas  
 351 correspond with other CFAs that were not included in the model (e.g., CFA # 77, 78, 80, 99, 94, 105,  
 352 and 107 for the Northeast Palawan round scad CFA and CFA # 53, 59, 69, and 73 for the Sulu sardine  
 353 CFA).



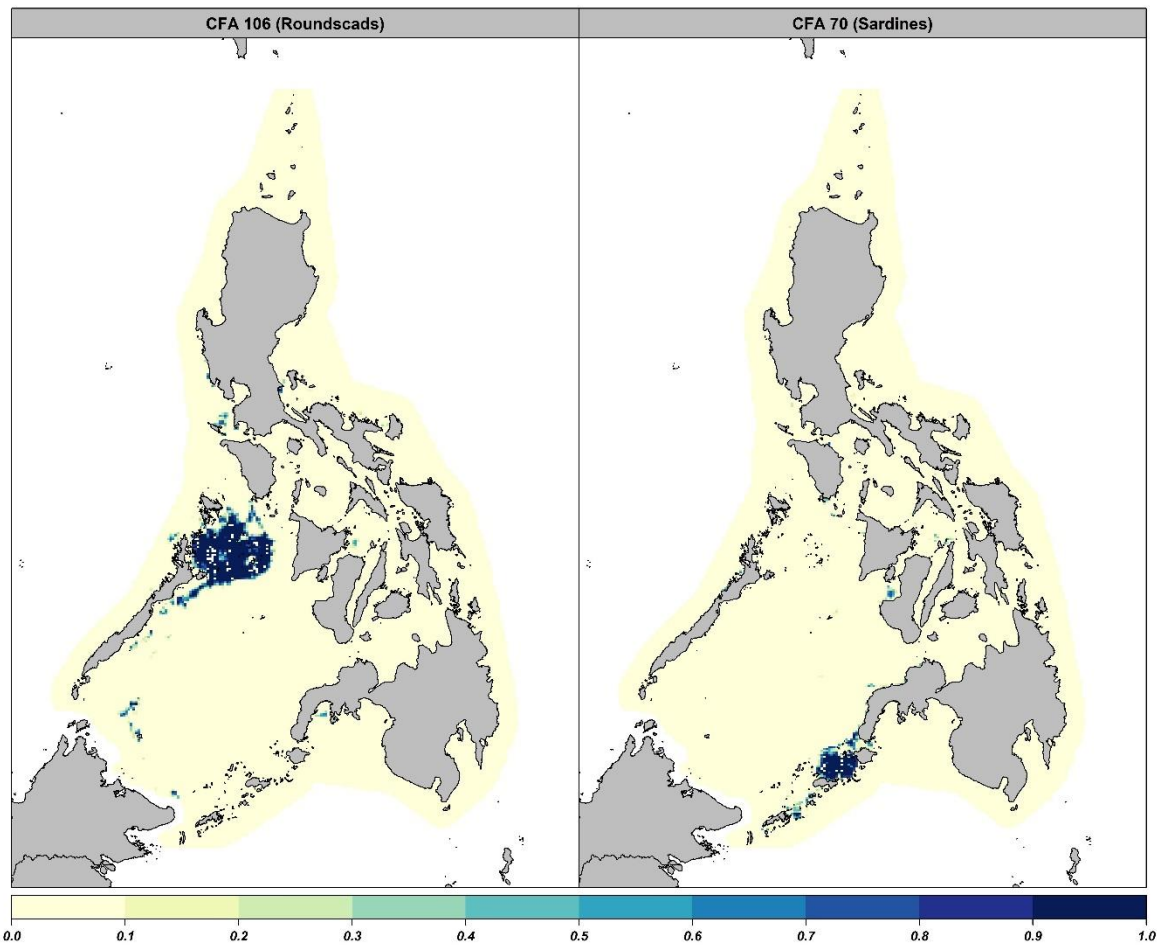
354

355

356

357

**Figure 9.** Predicted suitability maps for Core Fishing Areas for the different MaxEnt models developed using all VBD points inside the CFAs. Color scale represents degree of suitability relative to “typical” conditions found inside CFAs with 1 being highly suitable areas and 0 are unsuitable.



358

359 **Figure 10.** Predicted CFA suitability maps based on CFA # 106 (Northeast Palawan) and CFA # 70  
 360 (Sulu) representing predominantly round scad (*Decapterus sp.*) and sardine (*Sardinella lemuru*) fishing  
 361 grounds, respectively. Color scale represents degree of suitability relative to “typical” conditions  
 362 found inside CFAs with 1 being highly suitable areas and 0 are unsuitable.

#### 363 4. Discussion

364 The VIIRS nighttime imaging capabilities significantly enhanced those of the DMSP satellites,  
 365 particularly in terms of radiometric and spatial resolution, allowing for the nightly extraction of  
 366 locations and radiance information of maritime lights [21,30]. We applied this freely accessible and  
 367 novel dataset to identify, delineate, and characterize Core Fishing Areas (CFAs) and determine the  
 368 suitability of other parts of Philippine coastal waters to light-assisted fisheries and their target species.

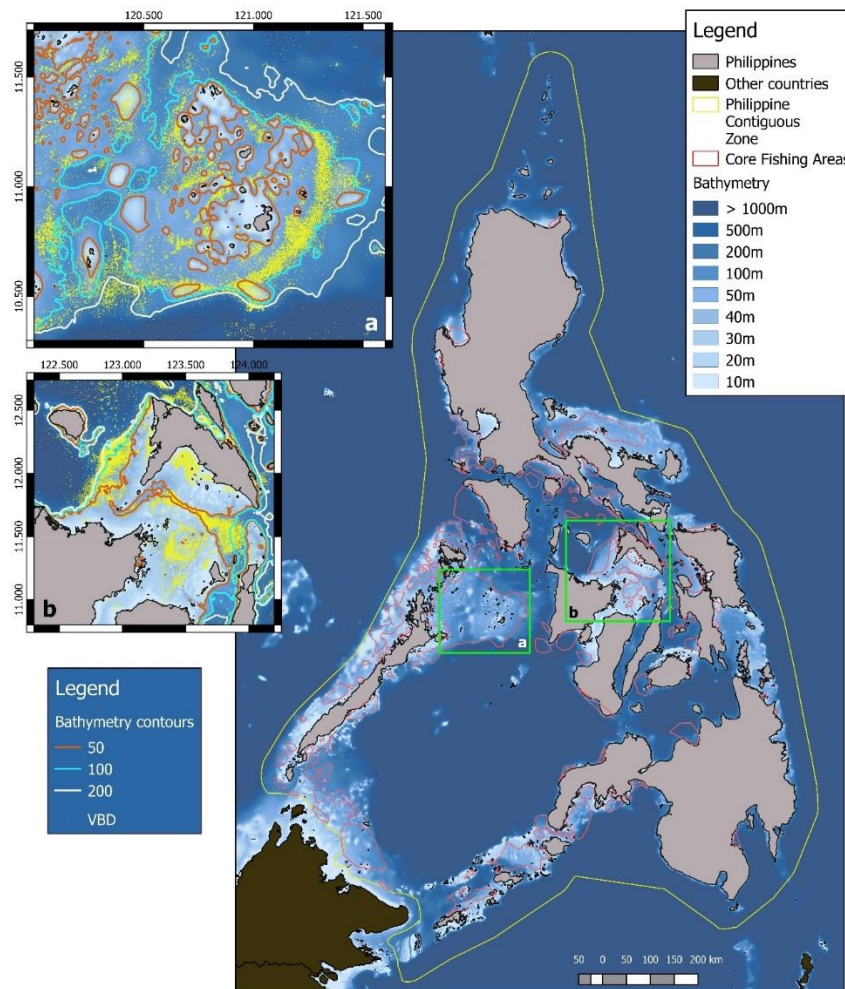
369 Many of the large CFAs identified are known primary fishing grounds for various coastal  
 370 pelagic fishes. The Sulu CFA (#70) in Southern Mindanao is dominated by sardine purse seine fishing.  
 371 It is one of the largest sources of the country’s sardine (*Sardinella lemuru*) supply and has been  
 372 subjected to seasonal fishery closures between November and March since 2011 due to concerns  
 373 about overfishing and stock declines [65]. The Northeast Palawan CFA (#106) and those west of  
 374 Palawan (e.g., CFAs # 102 to 117) are known round scad (*Decapterus macrosoma* and *Decapterus russelli*)  
 375 fishing areas, also subjected to annual seasonal closure since 2015 [66]. Visayan Sea 1 (#37) and 2 (#40)  
 376 CFAs are also part of a small pelagic fish seasonal closure established back in the 1970s primarily for  
 377 to sardines (*Sardinella gibbosa*).

378 Bathymetry, chlorophyll-a, and sea surface temperature have all been cited as predictors of small  
 379 pelagic fish spatial distribution in previous studies. Catches and fishing grounds for the Indian  
 380 mackerel (*Rastrelliger kanagurta*) in Indonesia correlated significantly with chlorophyll-a and sea  
 381 surface temperature [67]. Bottom depth and sea surface temperature explained variability in



382 European sardine (*Sardinella pilchardus*) presence in the Mediterranean Sea while bottom depth and  
 383 surface chlorophyll concentration predicted European anchovy (*Engraulis encrasicolus*) distribution  
 384 [68–70]. These three variables, along with salinity, are also used in mapping global distributions of  
 385 fish species through Aquamaps ([www.aquamaps.org](http://www.aquamaps.org)) [71,72]. These variables influence suitable  
 386 habitats for small pelagic fishes through zooplankton production and availability [73].

387 **Bathymetry consistently ranked highest in discriminating between CFA and non-CFA sites,**  
 388 **accounting for the most variability not captured in the other variables.** Chlorophyll accounted for  
 389 most of the variability in the MaxEnt model that excluded bathymetry indicating some correlation  
 390 between chlorophyll-a and bathymetry (Pearson’s correlation  $r = 0.25$ ;  $p < 0.01$ ). Indeed, chlorophyll-  
 391 a tend to decline with increasing depth. However, zooming in on some of the CFAs show how VBD  
 392 data track, with surprising precision, bathymetry and depth contours using the 1-km resolution  
 393 GEBCO bathymetry data (Figure 11). Removing bathymetry as a predictor resulted in lower accuracy  
 394 model (AUC from 0.88 to 0.86 and TSS from 0.59 to 0.55; Table 4) and broader predicted areas of  
 395 suitability (Figure 9). Aggregating data at a 4km resolution removes these fine-scale spatial patterns  
 396 in nighttime lights and fishing sites. Finer resolution environmental data could explain more of the  
 397 variability in the distribution of nighttime lights in CFAs. Unfortunately, current available monthly  
 398 remote sensing data for chlorophyll and sea surface temperatures for this region are limited to a 4-  
 399 km resolution (i.e., MODIS images) while finer oceanographic models are not available for the entire  
 400 study area.



401

402 **Figure 11.** CFAs overlay on a bathymetry map of the Philippines showing most of the CFAs are  
 403 located in less than 200 meter depths. Inset maps show how VBD points align with depth contours  
 404 for (a) Northeast Palawan and (b) Visayan Sea.



406

407

408

409

410

411

412

413

414

415

416

The dominance of bathymetry in distinguishing CFA from non-CFA sites could be attributed to (1) the depth preference of target species and (2) the multi-species nature of fisheries within CFAs. A quick search in Fishbase ([www.fishbase.org](http://www.fishbase.org)) on depth information for the dominant small pelagic fishes caught in Philippines waters shows that commonly targeted small pelagic fishes by Philippine fishing fleet are often found in depths of less than 200 meters [58]. In addition, CFAs most likely have a large mix of different fishing gears that target various species of small pelagic fishes. Since different species or species group tend to respond differently to water column characteristics (e.g., SST and chlorophyll-a concentrations), the common denominator in their environmental preference becomes bottom depth, a static variable which then gets captured as the main predictor of CFA versus non-CFA sites. If the CFAs could be differentiated according to their dominant target species, the effect of dynamic predictors in differentiating CFAs from non-CFAs for that particular species could be bigger than bathymetry.

417

418

419

420

421

422

423

424

425

426

427

428

429

430

431

432

433

434

435

436

One of the main uses of the identified Core Fishing Areas and habitat suitability map in this study is to delineate fisheries management areas as part of implementing Ecosystem Approaches to Fisheries Management (EAFM) [8,9]. While we have provided here a way to identify frequently visited fishing grounds and predict habitat suitability of non-fishing grounds based on nighttime lights activity and environmental attributes, delineation of meaningful fisheries management unit as part EAFM should be done in consultation with relevant stakeholders [2]. Some of the CFAs could be grouped into larger fisheries management areas based on similarities in their target species and fishing gears used. In the absence of actual fishing data available for each CFA, the seasonality of fishing activities and the distribution of VBD radiance values could be used as a proxy for these characteristics. For example, the northern Palawan CFAs (e.g., #102 to 117) can be grouped into one FMA since they share the same seasonality in fishing activities (during northeast monsoon; Figure 4) and radiance signature (Figure 5; see also Figure S6 for maps of the CFAs color-coded according to cluster membership). The CFAs west of Mindoro island (#s 122 to 125) could also be considered as a separate fisheries management area given their similarities in both seasonality of fishing activities (during northeast monsoon) and radiance signature (mostly low radiance values). Of course, other fishing activities and practices should also be considered in defining appropriate fisheries management areas since the VBD only covers fishing vessels that use lights to attract fish. As Jennings and Lee [2] stated, the ultimate delineation and definition of “fishing grounds” would be a societal decision of choosing cut-offs and satisfying potential trade-offs in the use of limited marine space.

437

438

439

440

441

442

443

444

445

446

447

448

449

450

The VBD data could also provide important information on the levels of fishing effort over time. The estimated number of fishing vessels using lights in the Philippines from the VBD data (~1,000) is most likely an underestimate since the VIIRS instrument takes only one image per night and for most nights, there is always a part of the country that is obscured by thick cloud cover. Summing up the maximum nightly VBD per CFA for selected larger, well-separated CFAs (i.e., #s 19, 66, 70, 75, 106, 122) already results in 925 estimated light boats or fishing vessels with on-board lights. In comparison, there are an estimated 6,371 commercial fishing vessels (i.e., 3 gross tons and heavier) in the country as of 2007 [74]. Despite this potential underestimation of absolute fishing effort, the quarterly pattern of nighttime fishing lights still tracks closely the national statistics of landed catches of small pelagic fish (Figure S5). Monthly VBD data show a secondary peak between the 3rd and 4th quarter of each year which is not captured in the quarterly landed catch data. This secondary peak in the VBD data is most likely associated with the varying seasonal patterns of fishing activities among CFAs with some CFAs' peak VBD counts occurring around this period (Figure 4). Subject to further ground validation, the temporal trends in VBD data could be used as a proxy for relative fishing effort at the national level for small pelagic fish catch, a key input for normalizing catch data.

451

#### 4.1. Limitations and future improvements

452

453

454

455

In using the VBD data for fisheries studies, additional filtering is needed to ensure that most of the data are fishing vessels. Although VBD use quality flags to identify non-vessel light sources in the data, it has no flags to distinguish fishing from non-fishing vessels (e.g., cargo ships, tankers, passenger ships, construction and mining-related temporary structures, among others). Navigation

456 routes are clearly seen from VBD overlays which correspond with known shipping lanes (e.g.,  
457 between Mindoro and Panay Islands; Sabah, Malaysia and Tawi-Tawi, Philippines; Figure 3 and S4).  
458 Major ports and mining areas also have high density aggregations of nighttime lights. It is possible  
459 that many of these lights are also fishing vessels but without ground validation, we decided to  
460 exclude them as Core Fishing Areas and in the MaxEnt modeling of suitable areas. Even though we  
461 removed some of these potential CFAs, the fishing ground suitability map produced from MaxEnt  
462 was still able to identify some of them as potential fishing grounds for small pelagic fishes based on  
463 similarities in typical ocean conditions to most of the CFAs where lights are found (Figure 3; e.g.,  
464 Northeast tip of Mindanao).

465 We ran the maximum entropy model under the assumption that areas where fishers often fish  
466 (e.g., CFAs) are also areas of high relative abundance for the target species group, in this case, small  
467 pelagic fishes, and that environmental factors can be used to predict habitat suitability [75]. At a  
468 resolution of 742 meters, it is surprising that many of the cells where nighttime lights are found in  
469 the last five years are revisited over the years. We hypothesized that environmental factors played a  
470 large role in the spatial structure of the nighttime lights, particularly these frequently-visited and  
471 high-density sites. However, other factors also influence fishers' decisions in selecting fishing  
472 grounds such as projected fishing costs, estimated risk, and adherence to traditional fishing grounds  
473 [76]. These are not captured in our model.

474 The utility of the VBD data in informing ecosystem approaches to fisheries management could  
475 be enhanced by studies that can identify the relationships between radiance values and fishing  
476 characteristics (e.g., fishing gear or strategy). This would help translate the VBD products from  
477 remote sensing outputs to the more common fisheries metrics (e.g., number of vessels, fishing gears,  
478 and/or species). Despite these limitations, having nightly information on distributions of light-  
479 assisted fishing activities freely accessible and available to fisheries managers partially fills the crucial  
480 spatial data gap for implementing ecosystem approaches to fisheries management.

## 481 5. Conclusions

482 Any marine resource management requires an understanding of the spatial and temporal  
483 patterns of both resource use and target resources and the underlying processes. Yet collecting  
484 information on spatial and temporal patterns of resource use at relevant scales for locally-adapted  
485 action remains sparse especially in marine fisheries in developing countries. We used the VIIRS Boat  
486 Detection data service from NOAA to identify high density fishing grounds and predict areas within  
487 the Philippines's contiguous zone with similar environmental conditions in aid of implementing  
488 ecosystem approaches to fisheries management. Nighttime lights are extensively detected in the  
489 Philippine coastal waters. These lights spatially cluster and we have identified 134 distinct Core  
490 Fishing Areas. Aggregating all boat detections inside CFAs, these areas are strongly distinguished  
491 from non-CFA areas mainly by bathymetry, owing most probably to the multi-gear nature of fishing  
492 and the varying fishing operation strategies employed within each CFA. In two of the largest CFAs  
493 which we know are each targeting round scads and sardines, variable importance in the MaxEnt  
494 models corresponded with environmental parameters previously known to be associated with these  
495 species occurrence, highlighting the potential model improvement if the catch composition and  
496 fishing fleets within each CFA can be characterized. In addition, using finer spatial resolution  
497 environmental predictors could enhance model precision and differentiate suitable fishing areas even  
498 within the same CFA.

499 The VIIRS Boat Detection data is provided freely and for public use. Its applications can be  
500 further expanded by conducting ground-truthing and calibration studies to relate VBD radiance  
501 values to common fishery statistics (e.g., number of vessels, types of vessels, comparative fishing  
502 effort based on boat size, etc.). But even with the current dataset, having nightly coverage of fishing  
503 activities, even if just a subset of the entire fishing sector, provides an invaluable data stream of  
504 fishing effort for data-deficient fisheries, especially in Southeast Asia. Our results could also be used  
505 as a basis for establishing fisheries management areas in the Philippines and our approach could be  
506 applied to other countries that have high numbers of light-employing fishing vessels.

507 **Supplementary Materials:** The following are available online at [www.mdpi.com/xxx/s1](http://www.mdpi.com/xxx/s1), Figure S1: Marine  
508 traffic density map, Figure S2: HDBSCAN parameter combination, Figure S3: Mean radiance versus percentage  
509 cloud cover and moon illumination, Figure S4: Mean climatology maps of environmental predictors, Figure S5:  
510 Comparison of VBD trend and reported quarterly production of small pelagic fish in the Philippines, Figure S6:  
511 Core Fishing Areas mapped according to seasonal and radiance clusters, Table S1: Characteristics of Core Fishing  
512 Areas.

513 **Author Contributions:** Conceptualization, Rollan C. Geronimo, Russell E. Brainard and Camilo Mora; Data  
514 curation, Christopher D. Elvidge and Mudjekeewis D. Santos; Formal analysis, Rollan C. Geronimo and Erik C.  
515 Franklin; Funding acquisition, Russell E. Brainard; Methodology, Rollan C. Geronimo, Erik C. Franklin,  
516 Christopher D. Elvidge, Mudjekeewis D. Santos, Roberto Venegas and Camilo Mora; Supervision, Camilo Mora;  
517 Writing – original draft, Rollan C. Geronimo; Writing – review & editing, Erik C. Franklin, Russell E. Brainard,  
518 Christopher D. Elvidge, Mudjekeewis D. Santos, Roberto Venegas and Camilo Mora.

519 **Acknowledgments:** We thank Raffy Ramiscal and regional offices of the Philippine’s Bureau of Fisheries and  
520 Aquatic Resources, the National Fisheries Research and Development Institute, and the National Stock  
521 Assessment Program for comments on the manuscript and sharing their knowledge about nighttime fishing  
522 practices during the various workshops conducted under the BFAR-USAID-NOAA Partnership Program. RCG  
523 was also supported by the East-West Center. We thank Melanie Abecassis for her comments and suggestions  
524 that improved our analyses.

525 **Conflicts of Interest:** The authors declare no conflict of interest. The funders had no role in the design of the  
526 study; in the collection, analyses, or interpretation of data; in the writing of the manuscript, and in the decision  
527 to publish the results.  
528



529 **References**

- 530 1. Booth, A. J. Incorporating the spatial component of fisheries data into stock assessment models. *ICES J. Mar.*  
531 *Sci.* **2000**, *57*, 858–865, doi:10.1006/jmsc.2000.0816.
- 532 2. Jennings, S.; Lee, J. Defining fishing grounds with vessel monitoring system data — Defining fishing  
533 grounds with vessel monitoring system data — Supplementary Data. **2012**, *69*, 51–63.
- 534 3. Tidd, A.; Brouwer, S.; Pilling, G. Shooting fish in a barrel? Assessing fisher-driven changes in catchability  
535 within tropical tuna purse seine fleets. *Fish Fish.* **2017**, 1–13, doi:10.1111/faf.12207.
- 536 4. Parnell, E. P.; Dayton, P. K.; Fisher, R. A.; Loarie, C. C.; Darrow, R. D. Spatial patterns of fishing effort off  
537 San Diego: implications for zonal management and ecosystem function. *Ecol. Appl.* **2010**, *20*, 2203–2222,  
538 doi:10.1890/09-1543.1.
- 539 5. Cabral, R. B.; Gaines, S. D.; Johnson, B. A.; Bell, T. W.; White, C. Drivers of redistribution of fishing and non-  
540 fishing effort after the implementation of a marine protected area network: *Ecol. Appl.* **2017**, *27*, 416–428,  
541 doi:10.1002/eap.1446.
- 542 6. Walters, C. Folly and fantasy in the analysis of spatial catch rate data. *Can. J. Fish. Aquat. Sci.* **2003**, *60*, 1433–  
543 1436, doi:10.1139/f03-152.
- 544 7. Lorenzen, K.; Steneck, R. S.; Warner, R. R.; Parma, A. M.; Coleman, F. C.; Leber, K. M. The spatial dimension  
545 of fisheries\_putting it all in place.pdf. *Bull. Mar. Sci.* **2010**, *86*, 169–177.
- 546 8. Heenan, A.; Pomeroy, R.; Bell, J.; Munday, P. L.; Cheung, W.; Logan, C.; Brainard, R.; Yang Amri, A.; Aliño,  
547 P. M.; Armada, N. B.; David, L. T.; Rivera-Guieb, R.; Green, S.; Jompa, J.; Leonardo, T.; Mamauag, S. S.;  
548 Parker, B.; Shackeroff, J.; Yasin, Z. A climate-informed, ecosystem approach to fisheries management. *Mar.*  
549 *Policy* **2015**, *57*, 182–192, doi:10.1016/j.marpol.2015.03.018.
- 550 9. Gorospe, K. D.; Michaels, W.; Pomeroy, R.; Elvidge, C.; Lynch, P.; Wongbusarakum, S.; Brainard, R. E. The  
551 mobilization of science and technology fisheries innovations towards an ecosystem approach to fisheries  
552 management in the Coral Triangle and Southeast Asia. *Mar. Policy* **2016**, *74*, 143–152,  
553 doi:10.1016/j.marpol.2016.09.014.
- 554 10. Stewart, K. R.; Lewison, R. L.; Dunn, D. C.; Bjorkland, R. H.; Kelez, S.; Halpin, P. N.; Crowder, L. B.  
555 Characterizing fishing effort and spatial extent of coastal fisheries. *PLoS One* **2010**, *5*,  
556 doi:10.1371/journal.pone.0014451.
- 557 11. Kroodsma, D. A.; Mayorga, J.; Hochberg, T.; Miller, N. A.; Boerder, K.; Ferretti, F.; Wilson, A.; Bergman, B.;  
558 White, T. D.; Block, B. A.; Woods, P.; Sullivan, B.; Costello, C.; Worm, B. Tracking the global footprint of  
559 fisheries. *Science (80-. )*. **2018**, *359*, 904–908, doi:10.1126/science.aao5646.
- 560 12. Mccauley, B. D. J.; Woods, P.; Sullivan, B.; Bergman, B.; Jablonicky, C.; Roan, A.; Hirshfi, M.; Boerder, K.  
561 Ending hide and seek at sea. *Science (80-. )*. **2016**, *351*, 1148–1150.
- 562 13. Fett, R. W. Fishing Fleet Activities Revealed by Night-Time Data from the Defense Meteorological Satellite  
563 Program. *Mar. Fish. Rev.* **1975**, *47*, 1972–1975.
- 564 14. Croft, T. Nighttime images of the earth from space. *Sci. Am.* **1978**, *239*, 86–98,  
565 doi:10.1038/scientificamerican0778-86.
- 566 15. Huang, Q.; Yang, X.; Gao, B.; Yang, Y.; Zhao, Y. Application of DMSP/OLS nighttime light images: A meta-  
567 analysis and a systematic literature review. *Remote Sens.* **2014**, *6*, 6844–6866, doi:10.3390/rs6086844.
- 568 16. Davies, T. W.; Duffy, J. P.; Bennie, J.; Gaston, K. J. The nature, extent, and ecological implications of marine  
569 light pollution. *Front. Ecol. Environ.* **2014**, *12*, 347–355.
- 570 17. Davies, T. W.; Duffy, J. P.; Bennie, J.; Gaston, K. J. Stemming the Tide of Light Pollution Encroaching into  
571 Marine Protected Areas. *Conserv. Lett.* **2016**, *9*, 164–171, doi:10.1111/conl.12191.

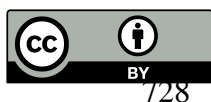
- 572 18. Elvidge, C. D.; Ziskin, D.; Baugh, K. E.; Tuttle, B. T.; Ghosh, T.; Pack, D. W.; Erwin, E. H.; Zhizhin, M. A  
573 fifteen year record of global natural gas flaring derived from satellite data. *Energies* **2009**, *2*, 595–622,  
574 doi:10.3390/en20300595.
- 575 19. Elvidge, C. D.; Zhizhin, M.; Baugh, K.; Hsu, F. C.; Ghosh, T. Methods for global survey of natural gas flaring  
576 from visible infrared imaging radiometer suite data. *Energies* **2016**, *9*, doi:10.3390/en9010014.
- 577 20. Miller, S. D.; Straka, W.; Mills, S. P.; Elvidge, C. D.; Lee, T. F.; Solbrig, J.; Walther, A.; Heidinger, A. K.; Weiss,  
578 S. C. Illuminating the capabilities of the suomi national Polar-orbiting partnership (NPP) visible infrared  
579 imaging radiometer suite (VIIRS) day/night Band. *Remote Sens.* **2013**, *5*, 6717–6766, doi:10.3390/rs5126717.
- 580 21. Elvidge, C. D.; Zhizhin, M.; Baugh, K.; Hsu, F. C. Automatic boat identification system for VIIRS low light  
581 imaging data. *Remote Sens.* **2015**, *7*, 3020–3036, doi:10.3390/rs70303020.
- 582 22. Straka, W. C.; Seaman, C. J.; Baugh, K.; Cole, K.; Stevens, E.; Miller, S. D. Utilization of the suomi national  
583 polar-orbiting partnership (npp) visible infrared imaging radiometer suite (viirs) day/night band for arctic  
584 ship tracking and fisheries management. *Remote Sens.* **2015**, *7*, 971–989, doi:10.3390/rs70100971.
- 585 23. Waluda, C. M.; Trathan, P. N.; Elvidge, C. D.; Hobson, V. R.; Rodhouse, P. G. Throwing light on straddling  
586 stocks of *Illex argentinus*: assessing fishing intensity with satellite imagery. *Can. J. Fish. Aquat. Sci.* **2002**, *59*,  
587 592–596, doi:10.1139/F02-049.
- 588 24. Kiyofuji, H.; Saitoh, S. I. Use of nighttime visible images to detect Japanese common squid *Todarodes*  
589 *pacificus* fishing areas and potential migration routes in the Sea of Japan. *Mar. Ecol. Prog. Ser.* **2004**, *276*, 173–  
590 186, doi:10.3354/meps276173.
- 591 25. Waluda, C. M.; Yamashiro, C.; Elvidge, C. D.; Hobson, V. R.; Rodhouse, P. G. Quantifying light-fishing for  
592 *Dosidicus gigas* in the eastern Pacific using satellite remote sensing. *Remote Sens. Environ.* **2004**, *91*, 129–133,  
593 doi:10.1016/j.rse.2004.02.006.
- 594 26. Saitoh, S.; Fukaya, a; Saitoh, K.; Semedi, B. Estimation of number of Pacific saury fishing vessels using  
595 night-time visible images. *ISPRS Arch.* **2010**, *Volume XXX*, 1013–1016.
- 596 27. Liu, Y.; Saitoh, S.-I.; Hirawake, T.; Igarashi, H.; Ishikawa, Y. Detection of Squid and a Pacific Saury fishing  
597 vessels around Japan using VIIRS Day/Night Band data. *Proc. Asia-Pacific Adv. Netw.* **2015**, *39*, 28–39,  
598 doi:10.7125/APAN.39.
- 599 28. Alabia, I. D.; Saitoh, S.; Mugo, R.; Igarashi, H.; Ishikawa, Y.; Usui, N.; Kamachi, M.; Awaji, T. Seasonal  
600 potential fishing ground prediction of neon flying squid (*Ommastrephes bartramii*) in the western and  
601 central North Pacific. **2015**, 190–203, doi:10.1111/fog.12102.
- 602 29. Syah, A. F.; Saitoh, S. I.; Alabia, I. D.; Hirawake, T. Predicting potential fishing zones for pacific saury  
603 (*Cololabis saira*) with maximum entropy models and remotely sensed data. *Fish. Bull.* **2016**, *114*, 330–342,  
604 doi:10.7755/FB.114.3.6.
- 605 30. Elvidge, C. D.; Baugh, K.; Zhizhin, M.; Hsu, F. C. Why VIIRS data are superior to DMSP for mapping  
606 nighttime lights. **2013**, 62–69.
- 607 31. Elvidge, C. D.; Ghosh, T.; Baugh, K.; Zhizhin, M. Rating the Effectiveness of Fishery Closures With Visible  
608 Infrared Imaging Radiometer Suite Boat Detection Data. *Front. Mar. Sci.* **2018**, *5*, 1–15,  
609 doi:10.3389/fmars.2018.00132.
- 610 32. Macusi, E. D.; Babaran, R. P.; van Zwieten, P. A. M. Strategies and tactics of tuna fishers in the payao  
611 (anchored FAD) fishery from general Santos city, Philippines. *Mar. Policy* **2015**, *62*, 63–73,  
612 doi:10.1016/j.marpol.2015.08.020.
- 613 33. Geronimo, R. C. *Small Fish , Big Impact: Dulong fisheries of San Juan, Batangas, Philippines: A Synthesis Report*;  
614 Conservation International: Quezon City, Philippines, 2013;

- 615 34. Dickson, J. O.; Alba, E. B.; Munprasit, A.; Chokesanguan, B.; Siriraksophon, S. *Fishing Gear and Methods in*  
616 *Southeast Asia: III. Philippines Part 2*; Ruangsivakul, N., Prajakjitt, P., Dickson, J. O., Siriraksophon, S., Eds.;  
617 Southeast Asian Fisheries Development, Training Department: Samutprakan, Thailand, 2003;
- 618 35. Hernando, a M. J.; Flores, E. E. C. The Philippines squid fishery: A review. *Mar. Fish. Rev.* **1981**, *43*, 13–20.
- 619 36. Zaragoza, E.; Pagdilao, C.; Moreno, E. Overview of small pelagic fisheries. In *In Turbulent Seas: The status of*  
620 *Philippine marine fisheries*; DA-BFAR (Department of Agriculture-Bureau of Fisheries and Aquatic  
621 Resources), Ed.; Coastal Resource Management Project: Cebu City, Philippines, 2004; p. 378.
- 622 37. Claus, S.; De Hauwere, N.; Vanhoorne, B.; Souza Dias, F.; Oset García, P.; Schepers, L.; Hernandez, F.; Mees,  
623 J. (Flanders Marine Institute). MarineRegions.org. Accessed at <http://www.marineregions.org> on 2016-08-  
624 05. 2016.
- 625 38. Jennings, S.; Dulvy, N. K. Reference points and reference directions for size-based indicators of community  
626 structure. *ICES J. Mar. Sci.* **2005**, *62*, 397–404, doi:10.1016/j.icesjms.2004.07.030.
- 627 39. Saul, S. E.; Walter, J. F.; Die, D. J.; Naar, D. F.; Donahue, B. T. Modeling the spatial distribution of  
628 commercially important reef fishes on the West Florida Shelf. *Fish. Res.* **2013**, *143*, 12–20,  
629 doi:10.1016/j.fishres.2013.01.002.
- 630 40. Campello, R. J. G. B.; Moulavi, D.; Sander, J. Density-Based Clustering Based on Hierarchical Density  
631 Estimates. In *Advances in Knowledge Discovery and Data Mining. PAKDD 2013. Lecture Notes in Computer*  
632 *Science, vol 7819*; Pei, J., Tseng, V. S., Cao, L., Motoda, H., Xu, G., Eds.; Springer: Berlin, Heidelberg, 2013;  
633 pp. 160–172 ISBN 978-3-642-37455-5.
- 634 41. R Core Team R: A language and environment for statistical computing. R Foundation for Statistical  
635 Computing, Vienna, Austria. Available online: <https://www.r-project.org/>.
- 636 42. McInnes, L.; Healy, J.; Astels, S. hdbscan: Hierarchical density based clustering. *J. Open Source Software, Open*  
637 *J.* **2017**, *2*.
- 638 43. Cao, C.; Bai, Y. Quantitative analysis of VIIRS DNB nightlight point source for light power estimation and  
639 stability monitoring. *Remote Sens.* **2014**, *6*, 11915–11935, doi:10.3390/rs61211915.
- 640 44. Irpino, A.; Verde, R. A New Wasserstein Based Distance for the Hierarchical Clustering of Histogram  
641 Symbolic Data. In *Data Science and Classification. Studies in Classification, Data Analysis, and Knowledge*  
642 *Organization*; Batagelj, V., Bock, H., Ferligoj, A., Žiberna, A., Eds.; Springer: Berlin, Heidelberg, 2006.
- 643 45. Irpino, A. HistDAWass: Histogram-Valued Data Analysis. R package version 1.0.1. [https://CRAN.R-](https://CRAN.R-project.org/package=HistDAWass)  
644 [project.org/package=HistDAWass](https://CRAN.R-project.org/package=HistDAWass) 2018.
- 645 46. Murtagh, F.; Legendre, P. Ward's Hierarchical Agglomerative Clustering Method: Which Algorithms  
646 Implement Ward's Criterion? *J. Classif.* **2014**, *31*, 274–295, doi:10.1007/s00357-.
- 647 47. Phillips, S. J.; Dudík, M.; Schapire, R. E. [Internet] Maxent software for modeling species niches and  
648 distributions (Version 3.4.1). Available from url:  
649 [http://biodiversityinformatics.amnh.org/open\\_source/maxent/](http://biodiversityinformatics.amnh.org/open_source/maxent/). Accessed on 2018-8-4. 2018.
- 650 48. Phillips, S. J.; Dudík, M. Modeling of species distribution with Maxent: new extensions and a comprehensive  
651 evaluation. *Ecography* **2008**, *31*, 161–175, doi:10.1111/j.2007.0906-7590.05203.x.
- 652 49. Morales, N. S.; Fernández, I. C.; Baca-González, V. MaxEnt's parameter configuration and small samples:  
653 are we paying attention to recommendations? A systematic review. *PeerJ* **2017**, *5*, e3093,  
654 doi:10.7717/peerj.3093.
- 655 50. Robinson, N. M.; Nelson, W. A.; Costello, M. J.; Sutherland, J. E.; Lundquist, C. J. A Systematic Review of  
656 Marine-Based Species Distribution Models (SDMs) with Recommendations for Best Practice. *Front. Mar. Sci.*  
657 **2017**, *4*, 1–11, doi:10.3389/fmars.2017.00421.

- 658 51. Elith, J.; Phillips, S. J.; Hastie, T.; Dudík, M.; Chee, Y. E.; Yates, C. J. A statistical explanation of MaxEnt for  
659 ecologists. *Divers. Distrib.* **2011**, *17*, 43–57, doi:10.1111/j.1472-4642.2010.00725.x.
- 660 52. Merino, G.; Barange, M.; Mullon, C. Climate variability and change scenarios for a marine commodity:  
661 Modelling small pelagic fish, fisheries and fishmeal in a globalized market. *J. Mar. Syst.* **2010**, *81*, 196–205,  
662 doi:10.1016/j.jmarsys.2009.12.010.
- 663 53. Zwolinski, J. P.; Emmett, R. L.; Demer, D. A. Predicting habitat to optimize sampling of Pacific sardine  
664 (*Sardinops sagax*). *ICES J. Mar. Sci.* **2011**, *68*, 867–879, doi:10.1093/icesjms/fsr038.
- 665 54. Peck, M. A.; Reglero, P.; Takahashi, M.; Catalán, I. A. Life cycle ecophysiology of small pelagic fish and  
666 climate-driven changes in populations. *Prog. Oceanogr.* **2013**, *116*, 220–245, doi:10.1016/j.pocean.2013.05.012.
- 667 55. Kaplan, I. C.; Williams, G. D.; Bond, N. A.; Hermann, A. J.; Siedlecki, S. A. Cloudy with a chance of sardines:  
668 Forecasting sardine distributions using regional climate models. *Fish. Oceanogr.* **2016**, *25*, 15–27,  
669 doi:10.1111/fog.12131.
- 670 56. Hijmans, R. J. raster: Geographic Data Analysis and Modeling. R package version 2.6-7. [https://CRAN.R-](https://CRAN.R-project.org/package=raster)  
671 [project.org/package=raster](https://CRAN.R-project.org/package=raster) 2017.
- 672 57. Thuiller, W.; Georges, D.; Engler, R.; Breiner, F. biomod2: Ensemble Platform for Species Distribution  
673 Modeling. R package version 3.3-15/r728. <https://R-Forge.R-project.org/projects/biomod/> 2017.
- 674 58. Trinidad, A. C.; Pomeroy, R. S.; Corpuz, P. V.; Agüero, M. *Bioeconomics of the Philippine small pelagics fishery*;  
675 ICLARM Tech Rep. 38, 1993;
- 676 59. Elith, J.; Leathwick, J. R. Species Distribution Models: Ecological Explanation and Prediction Across Space  
677 and Time. *Annu. Rev. Ecol. Evol. Syst.* **2009**, *40*, 677–697, doi:10.1146/annurev.ecolsys.110308.120159.
- 678 60. Elith, J.; Graham, C. H.; Anderson, R. P.; Dudík, M.; Ferrier, S.; Guisan, A.; Hijmans, R. J.; Huettmann, F.;  
679 Leathwick, J. R.; Lehmann, A.; Li, J.; Lohmann, L. G.; Loiselle, B. A.; Manion, G.; Moritz, C.; Nakamura, M.;  
680 Nakazawa, Y.; Overton, J. M.; Townsend Peterson, A.; Phillips, S. J.; Richardson, K.; Scachetti-Pereira, R.;  
681 Schapire, R. E.; Soberón, J.; Williams, S.; Wisz, M. S.; Zimmermann, N. E. Novel methods improve prediction  
682 of species' distributions from occurrence data. *Ecography (Cop.)*. **2006**, *29*, 129–151, doi:10.1111/j.2006.0906-  
683 7590.04596.x.
- 684 61. Phillips, S. J.; Anderson, R. P.; Schapire, R. E. Maximum entropy modeling of species geographic  
685 distributions. *Ecol. Modell.* **2006**, *190*, 231–259.
- 686 62. Thuiller, W.; Lafourcade, B.; Engler, R.; Araújo, M. B. BIOMOD - A platform for ensemble forecasting of  
687 species distributions. *Ecography (Cop.)*. **2009**, *32*, 369–373, doi:10.1111/j.1600-0587.2008.05742.x.
- 688 63. Landis, J. R.; Koch, G. G. The Measurement of Observer Agreement for Categorical Data. *Biometrics* **1977**,  
689 *33*, 159, doi:10.2307/2529310.
- 690 64. Phillips, S. J.; Anderson, R. P.; Dudík, M.; Schapire, R. E.; Blair, M. E. Opening the black box: an open-source  
691 release of Maxent. *Ecography (Cop.)*. **2017**, *40*, 887–893, doi:10.1111/ecog.03049.
- 692 65. Rola, A. C.; Narvaez, T. A.; Naguit, M. R. A.; Elazegui, D. D.; Brillo, B. B. C.; Paunlagui, M. M.; Jalotjot, H.  
693 C.; Cervantes, C. P. Impact of the closed fishing season policy for sardines in Zamboanga Peninsula,  
694 Philippines. *Mar. Policy* **2018**, *87*, 40–50, doi:10.1016/j.marpol.2017.09.029.
- 695 66. Diego, T.-J. A. S.; Fisher, W. L. Trends in the capture fisheries in Cuyo East Pass, Philippines. *Int. J. os Fish.*  
696 *Aquat. Stud.* **2014**, *1*, 57–72.
- 697 67. Nurdin, S.; Mustapha, M. A.; Lihan, T. The Relationship between Sea Surface Temperature and Chlorophyll-  
698 a Concentration in Fisheries Aggregation Area in the Archipelagic Waters of Spermonde Using Satellite  
699 Images. **2015**, *466*, doi:10.1063/1.4858699.
- 700 68. Bellido, J. M.; Brown, A. M.; Valavanis, V. D.; Giráldez, A.; Pierce, G. J.; Iglesias, M.; Palialexis, A. Identifying



- 701 essential fish habitat for small pelagic species in Spanish Mediterranean waters. *Hydrobiologia* **2008**, *612*, 171–  
702 184, doi:10.1007/s10750-008-9481-2.
- 703 69. Schismenou, E.; Tsoukali, S.; Giannoulaki, M.; Somarakis, S. Modelling small pelagic fish potential  
704 spawning habitats: eggs vs spawners and in situ vs satellite data. *Hydrobiologia* **2017**, *788*, 17–32,  
705 doi:10.1007/s10750-016-2983-4.
- 706 70. Tugores, P.; Giannoulaki, M.; Iglesias, M.; Bonanno, A.; Tičina, V.; Leonori, I.; MacHias, A.; Tsagarakis, K.;  
707 Díaz, N.; Giráldez, A.; Patti, B.; De Felice, A.; Basilone, G.; Valavanis, V. Habitat suitability modelling for  
708 sardine *Sardina pilchardus* in a highly diverse ecosystem: The Mediterranean Sea. *Mar. Ecol. Prog. Ser.* **2011**,  
709 *443*, 181–205, doi:10.3354/meps09366.
- 710 71. Kaschner, K.; Kesner-Reyes, K.; Garilao, C.; Rius-Barile, J.; Rees, T.; Froese, R. AquaMaps: Predicted range  
711 maps for aquatic species.
- 712 72. Kesner-Reyes, K.; Kaschner, K.; Kullander, S.; Garilao, C.; Baril, J.; Froese, R. AquaMaps: algorithm and  
713 data sources for aquatic organisms. *FishBase. World Wide Web Electron. Publ. www.fishbase.org, version* **2012**.
- 714 73. Saraux, C.; Fromentin, J.-M.; Bigot, J.-L.; Bourdeix, J.-H.; Morfin, M.; Roos, D.; Van Beveren, E.; Bez, N.  
715 Spatial Structure and Distribution of Small Pelagic Fish in the Northwestern Mediterranean Sea. *PLoS One*  
716 **2014**, *9*, e111211, doi:10.1371/journal.pone.0111211.
- 717 74. DA-BFAR *Philippine Fisheries Profile* 2012.  
718 [https://www.bfar.da.gov.ph/files/img/photos/2012FisheriesProfile\(Finalcopy\)\(1\).pdf](https://www.bfar.da.gov.ph/files/img/photos/2012FisheriesProfile(Finalcopy)(1).pdf); 2012;
- 719 75. Alabia, I. D.; Saitoh, S. I.; Hirawake, T.; Igarashi, H.; Ishikawa, Y.; Usui, N.; Kamachi, M.; Awaji, T.; Seito,  
720 M. Elucidating the potential squid habitat responses in the central North Pacific to the recent ENSO flavors.  
721 *Hydrobiologia* **2016**, *772*, 215–227, doi:10.1007/s10750-016-2662-5.
- 722 76. Girardin, R.; Hamon, K. G.; Pinnegar, J.; Poos, J. J.; Thébaud, O.; Tidd, A.; Vermard, Y.; Marchal, P. Thirty  
723 years of fleet dynamics modelling using discrete-choice models: What have we learned? *Fish Fish.* **2016**, 1–  
724 18, doi:10.1111/faf.12194.
- 725



© 2018 by the authors. Submitted for possible open access publication under the terms and conditions of the Creative Commons Attribution (CC BY) license (<http://creativecommons.org/licenses/by/4.0/>).